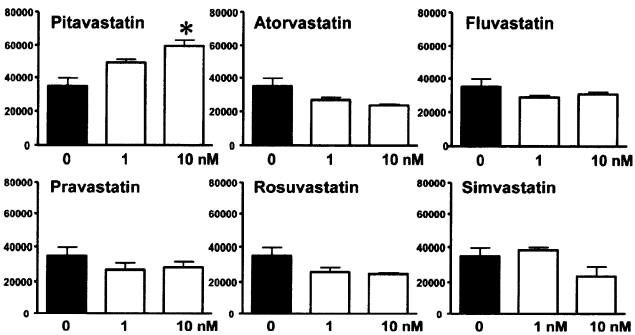

Fig 1. Effects of six statins on angiogenic capacity of human endothelial cells in vitro is shown by quantitative analysis of tube formation (tube length in mm per well) in six independent experiments. *$P < .01$ vs control by one-way analysis of variance with the Dunnett multiple comparison test.

artery and advanced to the left internal iliac artery at the level of the interspaces between the seventh lumbar and the first sacral vertebrae. After an intra-arterial injection of nitroglycerin (0.25 mg), 5 mL of contrast medium was injected at a rate of 1 mL/s. The 3-second angiogram was used for analysis of the angiographic score. A composite of 5-mm^2 grids was placed over the angiogram. The total number of grids that were crossed by visible arteries was divided by the total number of grids in the area of the medial thigh, as previously described.[21,22]

Capillary and arteriolar density. Histologic evaluation was performed for 5-μm frozen sections or 5-μm paraffin-embedded sections of the adductor skeletal muscles of the ischemic limb. CD31$^+$ (Dako, Tokyo, Japan) capillary endothelial cells were counted. Arterioles were determined by immunostaining with α-smooth muscle actin (α-SMA; Dako) and anti-mouse immunoglobulin G secondary antibody (Alexa 546; Molecular Probes, Invitrogen, Carlsbad, Calif), and vessels surrounded by smooth muscle cells were counted. Nuclei were counterstained with 4′,6-diamidino-2-phenylindole (Vector Shield, Vector Laboratories, Burlingame, Calif). Capillary and arteriolar density were calculated as capillaries/mm^2 and arterioles/mm^2 averaged from five randomly selected fields.[21,22] To ensure that the density was not overestimated or underestimated as a consequence of myocyte atrophy or edema, the capillary/muscle and arteriolar/muscle fiber ratios were also evaluated.

Tissue oximetry. Tissue oxygen content was measured by fluorescence quenching technique using an OxyLab PO_2 monitor (Oxford Optronix Ltd, Oxfordshire, UK) fiberoptic probe mounted to a micromanipulator, as previously described.[23] Ischemic limb was exposed on an anesthetized animal, and a 18-gauge needle was used to insert the fiberoptic probe to the adductor skeletal muscles of the ischemic limb at a 90° angle to contact the adductor skeletal muscles. The stable Po_2 reading, before a rapid rise to at least 60 mm Hg that signaled loss of tissue contact, was used as the tissue oxygen partial pressure.

Effects of pitavastatin-NP on forced ischemia induced by electrical pulses. The functional status of collateral arterial development was examined 28 days after treatment with PBS, FITC-NP, pitavastatin only, and pitavastatin-NP. After anesthesia, 21-gauge catheters were inserted into the right femoral artery and the left femoral vein for blood sampling. Two 21-gauge needles were inserted into the left medial thigh and the left gastrocnemius muscle. The electrode wires were then connected to the needles and plugged into the stimulator (Electronic Stimulator, Model SEN-7203, NIHON KOHDEN, Tokyo, Japan). The stimulating voltage was set at 5 V for 1 millisecond to cause noticeable contraction of the left hind limb. The stimulation frequency was 3 Hz, and the left hind limb was electrically stimulated for 30 minutes. Arterial and venous blood was sampled to measure the oxygen saturation before stimulation and at 15 and 30 minutes after stimulation.

A mouse model of hind limb ischemia and treatments. Male wild-type and Flt-1 tyrosine kinase deficient (Flt-1 TK$^{-/-}$) mice[24] were used. After anesthesia, unilateral hind limb ischemia was induced in the mice as previously described.[10,25] Additional details are provided in the Appendix (online only).

Statistical analyses. Data are expressed as mean ± standard error of the mean. Statistical analysis was assessed by one-way or two-way analysis of variance with post hoc test. Values of $P < .05$ were considered statistically significant.

RESULTS

Effects of statins and pitavastatin-NP on the angiogenic capacity of HECs in vitro. Treatment with pitavastatin increased angiogenic activity in HECs, whereas other statins had no effect (Fig 1). Treatment with pitavastatin-

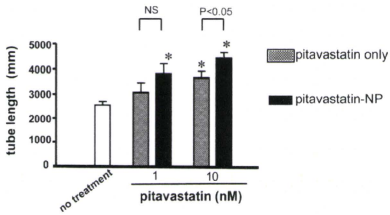

Fig 2. Effects of pitavastatin and pitavastatin nanoparticles *(NP)* are shown on the angiogenic capacity of human endothelial cells in vitro by quantitative analysis of tube formation (tube length per well) of six independent experiments. $*P < .01$ vs control by two-way analysis of variance with the Dunnett multiple comparison test.

NP increased angiogenic activity in HECs. The angiogenic activity of statin-NP was greater than that of 10 nM pitavastatin alone (Fig 2).

Effects of pitavastatin-NP on angiographically visible collateral arterial development. Because only a single dose of pitavastatin (0.4 mg/kg)-NP was previously examined in the mouse model,[13] the dose-response relationship of pitavastatin-NP with angiographically visible collateral arterial development (arteriogenesis) was examined in the present study. Treatment with pitavastatin (0.5 mg/kg)-NP, but not with those with pitavastatin at 0.05 or 0.15 mg/kg, increased the arteriogenic response, as assessed by the angiographic score (Fig 3, *A*). Representative angiograms 28 days after treatment demonstrate corkscrew-like collateral arterial development only in the pitavastatin-NP group (Fig 3, *B*). Treatment with pitavastatin (0.5 mg/kg)-NP significantly increased the angiographic score (Fig 3, *C*). In contrast, no treatment effects on the angiographic score were noted in the FITC-NP or pitavastatin-only groups.

Effects of pitavastatin-NP on histopathologic angiogenesis and arteriogenesis. Treatment with pitavastatin (0.5 mg/kg)-NP, but not with FITC-NP or statin only, significantly increased the capillary density and capillary/muscle fiber ratio, which are indices of angiogenesis (Fig 4, *A*). The beneficial effects of pitavastatin-NP were not associated with significant changes in serum biochemical markers (Table). Treatment with pitavastatin-NP also significantly increased the α-SMA$^+$ arteriolar density and arteriole/muscle fiber ratio, which are indices of arteriogenesis (Fig 4, *B*), indicating that pitavastatin-NP treatment induced angiogenesis and arteriogenesis.

Examination of hematoxylin-eosin-stained sections revealed no abnormal histopathologic findings (inflammation and fibrosis) among the four groups (data not shown). There was no significant difference in muscle fiber density among the four groups (PBS groups: 129 ± 8, 145 ± 4/mm^2; FITC-NP groups: 130 ± 3 and 129 ± 6/mm^2).

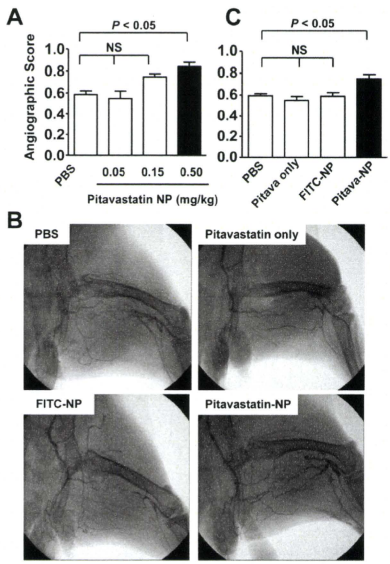

Fig 3. Effects of pitavastatin nanoparticles (*NP*) on angiographically visible collateral arterial development are shown 28 days after treatment. **A,** Effects of pitavastatin-NP containing 0.05, 0.15, or 0.5 mg/kg pitavastatin on the angiographic score (n = 3 each). **B,** Representative angiograms are shown of the phosphate buffered saline *(PBS)*, pitavastatin-only, fluorescein isothiocyanate *(FITC)*-NP, and pitavastatin-NP groups at 28 days after treatment. Corkscrew-like collateral arteries were observed only in the pitavastatin-NP group. **C,** Summary of the angiographic scores obtained for the four groups in panel **B** (n = 6 each).

Effects of pitavastatin-NP on tissue oxygen saturation. The tissue oxygen pressure in adductor skeletal muscles of the ischemic limb was measured 28 days after treatment. Treatment with pitavastatin (0.5 mg/kg)-NP significantly increased tissue oxygen pressure compared with the other groups (Appendix Fig II, online only).

Endothelial cell-selective delivery of NP. The cellular distribution of FITC was examined 3, 7, and 28 days after the intramuscular injection of FITC-NP or FITC only. On day 3 after injection, strong FITC signals were detected in FITC-NP–injected ischemic muscle (Fig 5, *A*), whereas no FITC signals were observed in control nonischemic muscle (Fig 5, *A*) or in ischemic muscle injected with FITC only (data not shown). The FITC signals were localized predominantly to the capillaries and arterioles. Weak FITC signals were also detected in myocytes at day 3t. On day 7 and 28, FITC signals remained localized predomi-

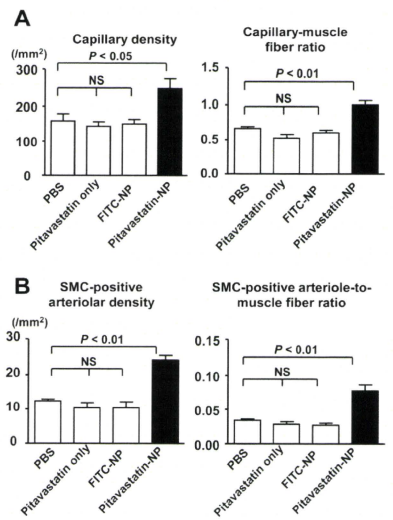

Fig 4. Effects of pitavastatin nanoparticles (*NP*) on angiogenesis and arteriogenesis are shown 28 days after treatment. **A,** CD-31$^+$ capillary density and capillary/muscle fiber ratio (indices of angiogenesis) is shown in ischemic muscles (n = 6 each). **B,** α-Smooth muscle actin (α-SMA)-positive arteriolar density and arteriole/muscle fiber ratio is shown in ischemic muscles (indices of arteriogenesis; n = 8 each). *FITC,* Fluorescein isothiocyanate; *PBS,* phosphate-buffered saline; *SMC,* smooth muscle cells.

nantly to capillaries and arterioles (Fig 5, *A*). Immunofluorescent staining revealed that FITC signals localized mainly to CD31$^+$ endothelial cells in FITC-NP–injected ischemic muscle 28 days after ischemia (Fig 5, *B*). In contrast, no FITC signals were observed in skeletal muscle myocytes on day 7 and 28 or in contralateral nonischemic hind limbs or remote organs (liver, spleen, kidney, and heart) at any time point (data not shown).

Effects of pitavastatin-NP on exercise-induced ischemia induced by electrical stimulation. To assess the functional efficacy of pitavastatin-NP on collateral arterial development, the effects of pitavastatin-NP on exercise-induced ischemia by electrical stimulation were examined. In the control PBS group, venous oxygen saturation in ischemic muscle decreased, and thus the difference in arteriovenous oxygen saturation increased after 15 and 30 minutes of electrical stimulation (Fig 6, *A*), suggesting the occurrence of exercise-induced ischemia. Treatment with pitavastatin-NP, but not with FITC-NP or pitavastatin only, abrogated the increase in arteriovenous oxygen difference in the ischemic limb (Fig 6, *B*). There were no significant differences in systemic blood hemoglobin levels among the four groups (data not shown).

Effects of vatalanib-NP on angiogenesis and arteriogenesis induced by pitavastatin-NP. We recently reported in a murine model that therapeutic neovascularization induced by pitavastatin-NP was mediated by increased eNOS activity and multiple endogenous angiogenic growth factors, such as VEGF.[10,25] Consequently, we examined VEGF expression in the four groups 28 days after treatment by immunohistochemistry and found increased VEGF positivity in CD31$^+$ endothelial cells of the capillaries and arterioles in the pitavastatin-NP group compared with other groups (Appendix Fig III, online only). Interestingly, positive VEGF staining was also detected in myocytes in the pitavastatin-NP group.

Vatalanib was selected because this molecule inhibits receptor tyrosine kinases of VEGR receptor types 1-3. Treatment with vatalanib-NP elicited no effects on angiographically visible collateral arterial development induced by hind limb ischemia in animals treated with PBS; however, it abrogated the arteriogenic response induced by pitavastatin-NP (Fig 7, *A* and *B*). In addition, treatment with vatalanib-NP abrogated histopathologic, angiogenic (capillary density), and arteriogenic (arteriolar density) responses induced by pitavastatin-NP (Fig 7, *C*). Vatalanib-NP elicited significant effects on histopathologic arteriogenic (arteriolar density) responses under baseline conditions (Fig 7, *C*).

Effects of pitavastatin-NP on angiogenesis and arteriogenesis in flt-1 TK$^{-/-}$ mice transfected with and without the *sFlt-1* gene. To examine the role of VEGF receptors (flk-1 and flt-1), the effects of pitavastatin-NP on ischemia-induced neovascularization were examined in wild-type and flt-1 TK$^{-/-}$ mice (Appendix Fig IV, online only). Compared with wild-type mice, the therapeutic effects of pitavastatin-NP decreased but were still observed in flt-1 TK$^{-/-}$ mice. To further examine the role of flk-1, *sFlt-1* gene transfer was performed into flt-1 TK$^{-/-}$ mice. The *sFlt-1* gene transfer blunted the therapeutic effects of pitavastatin-NP.

DISCUSSION

The present study demonstrates that NP-mediated endothelial cell-selective delivery of pitavastatin increased the development of collateral arteries (arteriogenesis) and improved exercise-induced ischemia in a rabbit model of chronic hind limb ischemia, indicating that this novel cell-selective delivery system is feasible for therapeutic arteriogenesis. We selected this rabbit model for translation to clinical settings in humans because it represents a preclinical model of arteriogenesis after femoral artery occlusion,[26] as observed in patients with severe peripheral artery disease.

Stimulation of the growth of collateral arteries (arteriogenesis) is evolving as a new therapeutic option for patients with atherosclerotic occlusive vascular disease, even though induction of additional angiogenesis or vasculogenesis is beneficial.[11,13] We assumed that the vascular endothelium would be an appropriate cellular target for the development

Table. Serum biochemical profiles

Variable[a]	*PBS*	*FITC-NP*	*Pitavastatin only*	*Pitavastatin-NP*
CPK (U/L)				
Day 7	345 ± 30	766 ± 270	445 ± 98	385 ± 44
Day 14	279 ± 8	486 ± 38	459 ± 118	296 ± 18
Day 21	242 ± 16	535 ± 58	396 ± 72	252 ± 12
Day 28	275 ± 60	229 ± 15	275 ± 33	259 ± 31
AST (IU/L)				
Day 7	10 ± 1	19 ± 3	16 ± 2	10 ± 1
Day 14	7 ± 0.3	19 ± 3	19 ± 6	8 ± 3
Day 21	15 ± 1	20 ± 2	22 ± 7	19 ± 4
Day 28	31 ± 11	29 ± 6	18 ± 2	20 ± 2
ALT (IU/L)				
Day 7	36 ± 9	36 ± 10	38 ± 5	29 ± 11
Day 14	26 ± 1	34 ± 6	37 ± 7	33 ± 9
Day 21	38 ± 7	33 ± 5	37 ± 8	43 ± 11
Day 28	42 ± 8	41 ± 10	35 ± 11	53 ± 19
BUN (mg/dl)				
Day 7	24 ± 0.2	17.3 ± 0.2	18 ± 1.5	24 ± 2
Day 14	23 ± 1	19.6 ± 2	24 ± 2	25 ± 1
Day 21	19 ± 1	18 ± 4	20 ± 2	19 ± 0.4
Day 28	26 ± 1	17 ± 0.3	17 ± 0.4	29 ± 2
Creatinine (mg/dL)				
Day 7	0.66 ± 0.01	0.82 ± 0.07	0.89 ± 0.01	0.80 ± 0.11
Day 14	0.70 ± 0.04	0.81 ± 0.09	0.87 ± 0.08	0.73 ± 0.05
Day 21	0.95 ± 0.02	0.80 ± 0.06	0.95 ± 0.01	1.03 ± 0.02
Day 28	0.85 ± 0.08	0.91 ± 0.06	0.86 ± 0.03	0.92 ± 0.03
Total cholesterol (mg/dL)				
Day 7	31 ± 10	31 ± 1	19 ± 5	46 ± 5
Day 14	26 ± 8	24 ± 3	19 ± 1	31 ± 4
Day 21	29 ± 10	18 ± 1	18 ± 3	32 ± 6
Day 28	18 ± 3	18 ± 2	21 ± 1	17 ± 2

ALT, Alanine aminotransferase; *AST,* aspartate transaminase; *BUN,* blood urea nitrogen; *CPK,* creatinine phosphokinase.
[a]Data are mean ± standard error of the mean (n = 3 each).

of collateral arteries after arterial occlusion because the endothelium plays a central role in the mechanism of arteriogenesis by expressing multiple growth factors and by recruiting monocytes and smooth muscle cells. We found that FITC signals were localized mainly to the vascular endothelium for up to 4 weeks after the injection of FITC-NP into ischemic skeletal muscles of rabbits in vivo, indicating that this NP-mediated delivery system may be useful as an innovative strategy for a therapy targeting endothelial cells. We recently reported that after cellular delivery of NP by endocytosis into endothelial cells, the PLGA NP escapes from the endosomal compartment to the cytoplasmic compartment and is retained in the cytoplasm, where release of the encapsulated drug occurs slowly in conjunction with the hydrolysis of PLGA.[10,27-29]

Daily administration of statins at high doses has been reported to augment arteriogenesis in normocholesterolemic rabbits.[6] These pleiotropic effects of statins are mediated through reduced levels of cholesterol biosynthesis pathway intermediates that serve as lipid attachments for post-translational modification (isoprenylation) of proteins, including Rho and Rac. Pitavastatin was selected as the NP compound because (1) pitavastatin elicited the most potent effects on the angiogenic activity of HECs in vitro compared with other statins, and (2) NP-mediated intracellular delivery of pitavastatin showed greater angiogenic activity of HECs compared with pitavastatin alone (Figs 1 and 2).

We also found in an in vivo rabbit model that (1) a single intramuscular injection of pitavastatin-NP increased the angiographic score in a dose-dependent manner, (2) pitavastatin (0.5 mg/kg) -NP significantly increased arteriogenesis and tissue oxygen pressure (tissue perfusion), and (3) the treatment of pitavastatin-NP increased immunoreactive VEGF expression selectively in vascular endothelial cells in the ischemic limb. Therefore, it is likely that that after NP-mediated endothelial delivery, pitavastatin is slowly released from the NP into the cytoplasm, resulting in significant therapeutic effects. Sata et al[8] reported that systemic daily administration of pitavastatin (1 mg/kg/day × 49 days = 49 mg/kg) has significant therapeutic effects in mice with hind limb ischemia. In our previous study, we reported the efficacy of pitavastatin (0.4 mg/kg)-NP in a murine model.[10] Therefore, at an approximately 100-fold lower dose, our NP-mediated delivery system is as effective as the cumulative systemic dose.

In clinical trials that examined the effects of a single vascular growth factor on peripheral and coronary artery disease, clinical end points such as increased exercise tolerance were negative or disappointing, although increased vascularity was noted.[14,15] It has been reported that limb hemodynamics, such as ankle-brachial index or muscle

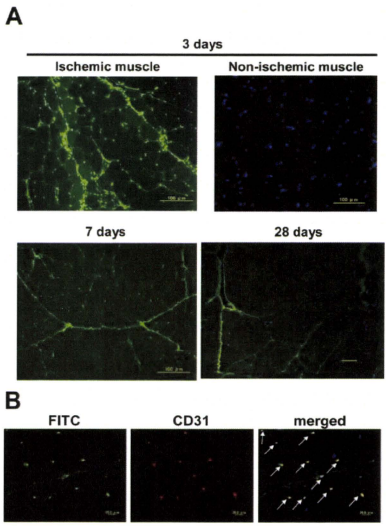

Fig 5. Cellular distribution of nanoparticles is shown in ischemic muscles. **A,** Fluorescent photomicrographs show cross sections of control nonischemic muscle and ischemic muscles at 3, 7, and 28 days after fluorescein isothiocyanate *(FITC)* nanoparticle *(NP)* injection. Nuclei were counterstained with 4′,6-diamidino-2-phenylindole *(blue)*. Fluorescence microscopic settings (exposure, filter, excitation light intensity, etc.) were the same for all images. Scale bar = 100 μm. **B,** Photomicrographs of cross sections of ischemic muscle 28 days after FITC-NP injection stained immunohistochemically with the endothelial marker CD31 *(red)*. Most FITC signals colocalized with the vascular endothelium *(arrows)*. Scale bars = 20 μm.

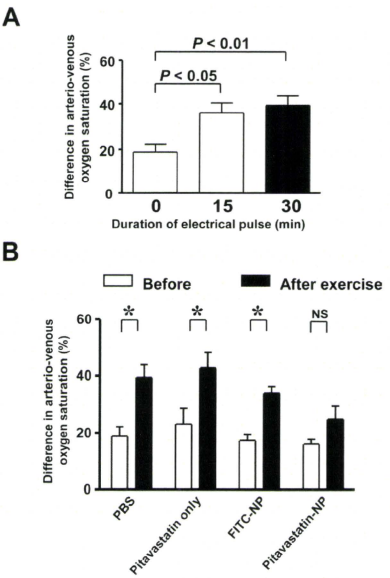

Fig 6. Effects are shown of pitavastatin nanoparticles *(NP)* on exercise-induced ischemia induced by electrical stimulation. **A,** Oxygen saturation in the femoral artery and vein in ischemic muscle is shown before and 15 and 30 minutes after muscular exercise by electrical stimulation in the phosphate-buffered saline *(PBS)* group (n = 6 each). **B,** The difference in arterial and venous oxygen saturation after 30 minutes of electrical pulse is shown in the four groups (n = 6 each). *FITC,* Fluorescein isothiocyanate.

blood flow at rest, are not correlated with functional capacity (claudication time or walking distance) in patients with peripheral arterial disease.[30] Therefore, assessment of the functional capacity of neovessels is needed in preclinical studies in animals. In other words, the improved functional capacity of collateral arteries must be a clinically important therapeutic goal in preclinical studies; however, few previous preclinical studies have addressed this point.

In the present study, we demonstrate that the arteriovenous oxygen difference in the ischemic hind limb increased in response to exercise in the PBS group, suggesting the development of exercised-induced ischemia. Treatment with pitavastatin-NP, but not with FITC-NP or pitavastatin only, prevented the development of exercise-induced ischemia. These data suggest that therapeutic arteriogenesis induced by pitavastatin-NP is associated with improved functional capacity.

We previously reported that the beneficial therapeutic effects induced by pitavastatin-NP are mediated by increased eNOS activity and multiple endogenous angiogenic growth factors in a murine model.[10] Recent reports by others have shown that mice lacking VEGF receptor 1 or placenta growth factor (a specific agonist of VEGR receptor 1), but not those lacking VEGF receptor 2, display impaired development of ischemia-induced angiogenesis and arteriogenesis.[31-33] However, roles of endogenous angiogenic growth factors in the mechanism of therapeutic effects of pitavastatin-NP have not been addressed.

In the present study, vatalanib-NP abrogated arteriogenic and angiogenic responses to pitavastatin-NP in rabbits. Furthermore, experiments with flt-1 $TK^{-/-}$ mice transfected with or without the *sFlt-1* gene showed partial contribution of both flt-1 and flk-1 to therapeutic angiogenic effects of pitavastatin-NP. These findings suggest that pitavastatin-NP produces an integrative system to form

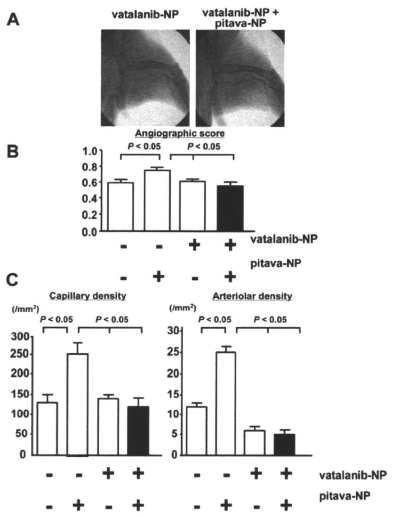

Fig 7. Effects of vatalanib nanoparticles *(NP)* are shown on angiogenesis and arteriogenesis induced by pitavastatin-NP. **A,** Representative angiograms show vatalanib-NP only and vatalanib-NP plus pitavastatin-NP groups 28 days after treatment. **B,** Summary of the angiographic scores obtained for the four groups (n = 3 each). **C,** Effects of vatalanib-NP are shown on histopathologic angiographic (capillary density) and arteriogenic (SMC-positive arteriolar density) responses induced by pitavastatin-NP.

functionally mature collaterals by controlled expression of endogenous VEGF and its receptor signals.

There are several limitations to the present study. First, only a single intramuscular injection of pitavastatin-NP was examined. In clinical settings, repetitive administration of an optimal dose may produce greater therapeutic effects. Second, we did not examine the contribution of bone marrow-derived progenitor cells because appropriate antibodies for detecting endothelial or smooth muscle progenitor cells are not available in rabbits. Further studies are needed to examine whether therapeutic effects afforded by pitavastatin-NP are associated with an increase in circulating endothelial progenitor cells.

CONCLUSIONS

This nanotechnology platform for vascular endothelial cell-selective delivery of pitavastatin is a promising strategy for the treatment of patients with severe organ ischemia and represents a significant advance in therapeutic arteriogenesis over current approaches. The nanotechnology platform may be further developed as a more effective and safer approach for therapeutic neovascularization.

AUTHOR CONTRIBUTIONS

Conception and design: SO, KE
Analysis and interpretation: SO, RN, KN, KE
Data collection: SO, RN, KN, KE
Writing the article: SO, KN, TM, KE
Critical revision of the article: SO, RN, KN, KE
Final approval of the article: SO, RN, KN, TM, MK, KS, RT, KE
Statistical analysis: SO, KN, KE
Obtained funding: KE
Overall responsibility: SO, KE

REFERENCES

1. Takemoto M, Liao JK. Pleotropic effects of 3-hydroxy-3-methylglutaryl coenzyme a reductase inhibitors. Arterioscler Thromb Vasc Biol 2001; 21:1712-9.
2. Egashira K, Hirooka Y, Kai H, Sugimachi M, Suzuki S, Inou T, et al. Reduction in serum cholesterol with pravastatin improves endothelium-dependent coronary vasomotion in patients with hypercholesterolemia. Circulation 1994;89:2519-24.
3. Ni W, Egashira K, Kataoka C, Kitamoto S, Koyanagi M, Inoue S, et al. Antiinflammatory and antiarteriosclerotic actions of HMG-CoA reductase inhibitors in a rat model of chronic inhibition of nitric oxide synthesis. Circ Res 2001;89:415-21.
4. Dimmeler S, Aicher A, Vasa M, Mildner-Rihm C, Adler K, Tiemann M, et al. HMG-CoA reductase inhibitors (statins) increase endothelial progenitor cells via the PI 3-kinase/Akt pathway. J Clin Invest 2001; 108:391-7.
5. Llevadot J, Murasawa S, Kureishi Y, Uchida S, Masuda H, Kawamoto A, et al. HMG-CoA reductase inhibitor mobilizes bone marrow—derived endothelial progenitor cells. J Clin Invest 2001;108:399-405.
6. Kureishi Y, Luo Z, Shiojima I, Bialik A, Fulton D, Lefer DJ, et al. The HMG-CoA reductase inhibitor simvastatin activates the protein kinase Akt and promotes angiogenesis in normocholesterolemic animals. Nat Med 2000;6:1004-10.
7. Kitamoto S, Nakano K, Hirouchi Y, Kohjimoto Y, Kitajima S, Usui M, et al. Cholesterol-lowering independent regression and stabilization of atherosclerotic lesions by pravastatin and by antimonocyte chemoattractant protein-1 therapy in nonhuman primates. Arterioscler Thromb Vasc Biol 2004;24:1522-8.
8. Sata M, Nishimatsu H, Osuga J, Tanaka K, Ishizaka N, Ishibashi S, et al. Statins augment collateral growth in response to ischemia but they do not promote cancer and atherosclerosis. Hypertension 2004;43:1214-20.
9. Zbinden S, Brunner N, Wustmann K, Billinger M, Meier B, Seiler C. Effect of statin treatment on coronary collateral flow in patients with coronary artery disease. Heart 2004;90:448-9.
10. Kubo M, Egashira K, Inoue T, Koga J, Oda S, Chen L, et al. Therapeutic neovascularization by nanotechnology-mediated cell-selective delivery of pitavastatin into the vascular endothelium. Arterioscler Thromb Vasc Biol 2009;29:796-801.
11. Schaper W, Scholz D. Factors regulating arteriogenesis. Arterioscler Thromb Vasc Biol 2003;23:1143-51.
12. Isner JM. Myocardial gene therapy. Nature 2002;415:234-9.
13. Heil M, Schaper W. Influence of mechanical, cellular, and molecular factors on collateral artery growth (arteriogenesis). Circ Res 2004;95: 449-58.
14. Losordo DW, Dimmeler S. Therapeutic angiogenesis and vasculogenesis for ischemic disease. Part I: angiogenic cytokines. Circulation 2004;109:2487-91.
15. Losordo DW, Dimmeler S. Therapeutic angiogenesis and vasculogenesis for ischemic disease: part II: cell-based therapies. Circulation 2004; 109:2692-7.
16. Ohtani K, Egashira K, Hiasa K, Zhao Q, Kitamoto S, Ishibashi M, et al. Blockade of vascular endothelial growth factor suppresses experimental restenosis after intraluminal injury by inhibiting recruitment of monocyte lineage cells. Circulation 2004;110:2444-52.

17. Zhao Q, Egashira K, Hiasa K, Ishibashi M, Inoue S, Ohtani K, et al. Essential role of vascular endothelial growth factor and Flt-1 signals in neointimal formation after periadventitial injury. Arterioscler Thromb Vasc Biol 2004;24:2284-9.
18. Zhao Q, Ishibashi M, Hiasa K, Tan C, Takeshita A, Egashira K. Essential role of vascular endothelial growth factor in angiotensin II-induced vascular inflammation and remodeling. Hypertension 2004;44:264-70.
19. Carmeliet P, Jain RK. Angiogenesis in cancer and other diseases. Nature 2000;407:249-57.
20. Wood JM, Bold G, Buchdunger E, Cozens R, Ferrari S, Frei J, et al. PTK787/ZK 222584, a novel and potent inhibitor of vascular endothelial growth factor receptor tyrosine kinases, impairs vascular endothelial growth factor-induced responses and tumor growth after oral administration. Cancer Res 2000;60:2178-89.
21. Kobayashi K, Kondo T, Inoue N, Aoki M, Mizuno M, Komori K, et al. Combination of in vivo angiopoietin-1 gene transfer and autologous bone marrow cell implantation for functional therapeutic angiogenesis. Arterioscler Thromb Vasc Biol 2006;26:1465-72.
22. Takeshita S, Zheng LP, Brogi E, Kearney M, Pu LQ, Bunting S, et al. Therapeutic angiogenesis. A single intraarterial bolus of vascular endothelial growth factor augments revascularization in a rabbit ischemic hind limb model. J Clin Invest 1994;93:662-70.
23. Babu AN, Murakawa T, Thurman JM, Miller EJ, Henson PM, Zamora MR, et al. Microvascular destruction identifies murine allografts that cannot be rescued from airway fibrosis. J Clin Invest 2007;117:3774-85.
24. Koga J, Matoba T, Egashira K, Kubo M, Miyagawa M, Iwata E, et al. Soluble Flt-1 gene transfer ameliorates neointima formation after wire injury in flt-1 tyrosine kinase-deficient mice. Arterioscler Thromb Vasc Biol 2009;29:458-64.
25. Hiasa K, Ishibashi M, Ohtani K, Inoue S, Zhao Q, Kitamoto S, et al. Gene transfer of stromal cell-derived factor-1alpha enhances ischemic vasculogenesis and angiogenesis via vascular endothelial growth factor/endothelial nitric oxide synthase-related pathway: next-generation chemokine therapy for therapeutic neovascularization. Circulation 2004;109:2454-61.
26. Hoefer IE, van Royen N, Buschmann IR, Piek JJ, Schaper W. Time course of arteriogenesis following femoral artery occlusion in the rabbit. Cardiovasc Res 2001;49:609-17.
27. Nakano K, Egashira K, Masuda S, Funakoshi K, Zhao G, Kimura S, et al. Formulation of nanoparticle-eluting stents by a cationic electrodeposition coating technology efficient nano-drug delivery via bioabsorbable polymeric nanoparticle-eluting stents in porcine coronary arteries. JACC Cardiovasc Interv 2009;2:277-83.
28. Kimura S, Egashira K, Nakano K, Iwata E, Miyagawa M, Tsujimoto H, et al. Local delivery of imatinib mesylate (STI571)-incorporated nanoparticle ex vivo suppresses vein graft neointima formation. Circulation 2008;118:S65-70.
29. Kimura S, Egashira K, Chen L, Nakano K, Iwata E, Miyagawa M, Tsujimoto H, et al. Nanoparticle-mediated delivery of nuclear factor kappaB decoy into lungs ameliorates monocrotaline-induced pulmonary arterial hypertension. Hypertension 2009;53:877-83.
30. Hiatt WR, Regensteiner JG, Hargarten ME, Wolfel EE, Brass EP. Benefit of exercise conditioning for patients with peripheral arterial disease. Circulation 1990;81:602-9.
31. Clayton JA, Chalothorn D, Faber JE. Vascular endothelial growth factor-A specifies formation of native collaterals and regulates collateral growth in ischemia. Circ Res 2008;103:1027-36.
32. Pipp F, Heil M, Issbrucker K, Ziegelhoeffer T, Martin S, van den Heuvel J, et al. VEGFR-1-selective VEGF homologue PlGF is arteriogenic: evidence for a monocyte-mediated mechanism. Circ Res 2003;92:378-85.
33. Nishi J, Minamino T, Miyauchi H, Nojima A, Tateno K, Okada S, et al. Vascular endothelial growth factor receptor-1 regulates postnatal angiogenesis through inhibition of the excessive activation of Akt. Circ Res 2008;103:261-8.

Submitted Aug 19, 2009; accepted Mar 10, 2010.

Additional online materials and results for this article may be found online at www.jvascsurg.org.

Circulation Journal
Official Journal of the Japanese Circulation Society
http://www.j-circ.or.jp

REVIEW

Oxidative Stress and Central Cardiovascular Regulation

– Pathogenesis of Hypertension and Therapeutic Aspects –

Yoshitaka Hirooka, MD; Yoji Sagara, MD; Takuya Kishi, MD; Kenji Sunagawa, MD

Oxidative stress is a key factor in the pathogenesis of hypertension and target organ damage, beginning in the earliest stages. Extensive evidence indicates that the pivotal role of oxidative stress in the pathogenesis of hypertension is due to its effects on the vasculature in relation to the development of atherosclerotic processes. It remains unclear, however, whether oxidative stress in the brain, particularly the autonomic nuclei (including the vasomotor center), has an important role in the occurrence and maintenance of hypertension via activation of the sympathetic nervous system. The aim of the present review is to describe the contribution of oxidative stress in the brain to the neural mechanisms that underlie hypertension, and discuss evidence that brain oxidative stress is a potential therapeutic target. (*Circ J* 2010; **74:** 827–835)

Key Words: Blood pressure; Brain; Heart rate; Hypertension; Sympathetic nervous system

Accumulating evidence indicates that the sympathetic nervous system plays an important role in the pathogenesis of hypertension.[1–3] Activation of the sympathetic nervous system is involved in the stages, clinical forms, 24-h blood pressure patterns, end-organ damage, and metabolic abnormalities of hypertension.[1–3] Although peripheral factors are also involved, the central nervous system (CNS) mechanisms are considered crucial.[3–7] The results of recent studies strongly suggest that central sympathetic outflow is increased in hypertension.[3–7] Increased oxidative stress is also involved in the pathogenesis of hypertension.[8] Although there have been many studies regarding target organ damage in hypertension, relatively few studies have addressed the role of oxidative stress in sympathetic nervous system activation.[9–11] Based on the role of angiotensin II (Ang II) in the generation of reactive oxygen species (ROS), the relationship between brain angiotensin and central sympathetic outflow has been examined.[12,13] Our group was the first to report that increased ROS generation in the brainstem contributes to the neural mechanisms of hypertension in hypertensive rats,[14] and we and other investigators have reported additional evidence to support this concept and the potential therapeutic aspects.[9–11] This review focuses on the role of oxidative stress within the brain in the neural pathogenesis of hypertension.

Increased Oxidative Stress in the Brain in Hypertension

Among the target organs of hypertensive vascular diseases, the brain is most affected by aging and oxidative stress.[15,16] Cell membranes in the brain contain a high concentration of polyunsaturated fatty acids. These fatty acids are targeted by ROS, which elicit chain reactions of lipid peroxidation. Oxidative stress is determined by measuring levels of thiobarbituric acid-reactive substances (TBARS), end products of lipid peroxidation. The levels of TBARS reflect those of malondialedehyde, although the assay is not specific for malondialedehyde.[15,17] There are some important points, however, for assessing the levels of TBARS.[17] The medium used for tissue preparation needs to contain a chelating agent and an antioxidant, and conditions for the assay must be kept constant. Therefore, we used another method for assessing the ROS production, which is electron spin resonance (ESR) spectroscopy. The amount of ROS was quantified by monitoring the time-dependent decay of the amplitude of the ESR spectra produced by the nitroxide radical 4-hydroxy-2,2,6,6-tetramethyl-piperidine-*N*-oxyl (hydroxyl-TEMPO) as a spin probe.[9,14] The signal decay of ESR spectroscopy reflects oxidative stress more directly. Also, it has an advantage for in vivo study.[18] We evaluated oxidative stress in the brains of stroke-prone spontaneously hypertensive rats (SHRSP) compared with normotensive Wistar–Kyoto (WKY) rats.[9,14] The rostral ventrolateral medulla (RVLM) is the major vasomotor center that determines basal sympathetic nervous system activity and it is essential for the maintenance of basal vasomotor tone.[3–7] Spontaneously hypertensive rats (SHR) or SHRSP exhibit increased sympathetic nervous system activity during the development of hypertension and are commonly used in experimental studies as models of human essential hypertension.[3–7] We previously investigated whether ROS are increased in the RVLM of SHRSP.[14] First, we found that ROS levels measured by TBARS and ESR spectroscopy were increased in the RVLM of SHRSP compared with WKY

Received February 19, 2010; revised manuscript received March 25, 2010; accepted March 26, 2010; released online April 15, 2010
Department of Cardiovascular Medicine, Kyushu University Graduate School of Medical Sciences, Fukuoka, Japan
Mailing address: Yoshitaka Hirooka, MD, Department of Cardiovascular Medicine, Kyushu University Graduate School of Medical Sciences, 3-1-1 Maidashi, Higashi-ku, Fukuoka 812-8582, Japan. E-mail: hyoshi@cardiol.med.kyushu-u.ac.jp
ISSN-1346-9843 doi:10.1253/circj.CJ-10-0153

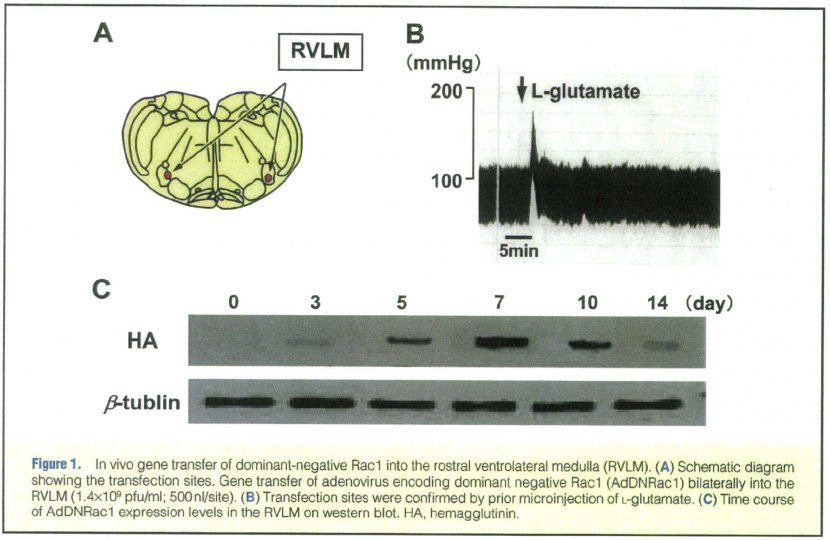

Figure 1. In vivo gene transfer of dominant-negative Rac1 into the rostral ventrolateral medulla (RVLM). (**A**) Schematic diagram showing the transfection sites. Gene transfer of adenovirus encoding dominant negative Rac1 (AdDNRac1) bilaterally into the RVLM (1.4×10^9 pfu/ml; 500 nl/site). (**B**) Transfection sites were confirmed by prior microinjection of L-glutamate. (**C**) Time course of AdDNRac1 expression levels in the RVLM on western blot. HA, hemagglutinin.

rats. In addition, superoxide dismutase (SOD) expression and activity, which are ROS scavenging factors, were decreased in the RVLM of SHRSP compared with WKY rats. Functionally, microinjection of the membrane-permeable radical scavenger tempol into the RVLM decreased blood pressure, heart rate, and sympathetic nervous system activity in SHRSP but not in WKY rats. More importantly, overexpression of Mn-SOD, an antioxidant enzyme, in the RVLM of SHRSP decreased blood pressure and sympathetic nervous system activity. These findings strongly indicate that oxidative stress in the RVLM is increased in SHRSP and contributes to the neural mechanisms of hypertension. As described here, brain ROS is one of the results of generalized target organ damage, appearing earlier in the brain due to its susceptibility. The brain ROS would increase blood pressure via activation of the sympathetic nervous system and this would ultimately result in a vicious cycle. It would be possible, however, that brain ROS is involved in the early stage of hypertension in SHR or SHRSP, because we found that oxidative stress in the brain assessed on in vivo ESR was enhanced in young (6-week-old) SHR or SHRSP compared with age-matched WKY rats (unpublished data). The levels of TBARS were not different, probably because the levels of TBARS reflect lipid peroxidation caused by ROS. Other investigators also found that an increase in superoxide anions in the RVLM is associated with hypertension in SHR,[19] and reduced expression and activity in Cu/Zn-SOD and Mn-SOD within the RVLM contribute to oxidative stress and neurogenic hypertension in SHR.[20] An increase in oxidative stress within the RVLM also plays an important role in maintaining high arterial blood pressure and sympathetic activation in 2-kidney 1-clip (2K-1C) hypertensive rats, which is a renovascular hypertension model.[21] In that study, Oliveira-Sales et al demonstrated that the mRNA expression of NAD(P)H oxidase subunits ($p47^{phox}$ and $gp91^{phox}$) in the RVLM was greater in 2K-1C than in the control group. Interestingly, there were no differences in Cu/Zn-SOD expression between the two groups. TBARS levels in the RVLM were significantly greater in the 2K-1C than in the control group, suggesting enhanced oxidative stress. Functionally, microinjection of vitamin C into the RVLM decreased blood pressure and renal sympathetic nerve activity in 2K-1C but not in controls. Importantly, in a subsequent study, these authors suggested that the paraventricular nucleus of the hypothalamus is also involved.[22] Notably, although 2K-1C is a model of renovascular hypertension, suggesting that circulating Ang II is increased, angiotensin type I (AT1) receptor gene expression levels within the RVLM and paraventricular nucleus were upregulated in this model, indicating that ROS was produced via the activation of nicotinamide-adenine dinucleotide phosphate [NAD(P)H] oxidase.

Sources of ROS Production in the Brain

As a source of ROS production in the CNS, NAD(P)H oxidase is a major player. NAD(P)H oxidase is composed of two membrane-bound subunits, $gp91^{phox}$ and $p22^{phox}$; several cytoplasmic subunits, $p47^{phox}$, $p40^{phox}$, and $p67^{phox}$; and the small G-protein Rac1.[23–26] Stimulation of AT1 receptors activates NAD(P)H oxidase by which the cytoplasmic subunits of Rac1NAD(P)H oxidase such as Rac1 bind to the membrane subunits, thereby activating the enzyme leading to superoxide generation. Rac1 requires lipid modification to migrate from the cytosol to the plasma membrane, which is a necessary step for activating ROS-generating NAD(P)H oxidase. NAD(P)H oxidase activity is greater in the brainstem of SHRSP than in that of WKY.[27,28] We transfected adenovirus

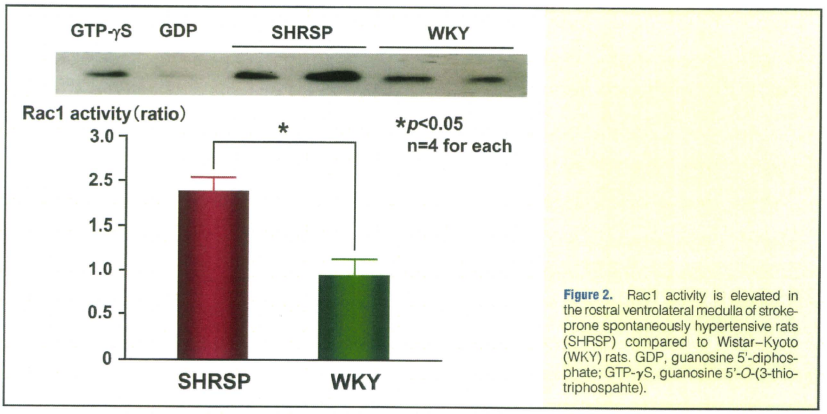

Figure 2. Rac1 activity is elevated in the rostral ventrolateral medulla of stroke-prone spontaneously hypertensive rats (SHRSP) compared to Wistar–Kyoto (WKY) rats. GDP, guanosine 5'-diphosphate; GTP-γS, guanosine 5'-*O*-(3-thiotriphosphahte).

encoding dominant-negative Rac1 into the RVLM of SHRSP and WKY rats (Figure 1).[27] Rac1 activity in the RVLM tissue was increased in SHRSP compared to WKY rats (Figure 2).[27] Importantly, we demonstrated that inhibition of Rac1-derived ROS in the RVLM decreased blood pressure, heart rate, and urinary norepinephrine excretion in SHRSP (Figure 3).[27] A similar response occurs after inhibition of Rac1-derived ROS in the nucleus tractus solitarius (NTS).[28]

In addition to the cytosolic production of ROS, mitochondria are the primary source of ROS production in many cells. Ang II increases mitochondrial ROS production in the RVLM, leading to sympathoexcitation.[29] Furthermore, NAD(P)H oxidase-derived ROS might trigger Ca^{2+} accumulation, which leads to mitochondrial ROS production.[29] This suggestion is based on the finding that gene transfer of dominant negative Rac1 attenuated the Ang II-induced increase in reduced Mito-Tracker red fluorescence.[29] In contrast, impairment of mitochondrial electron transport chain complexes in the RVLM might be involved in the neural abnormality underlying hypertension in SHR.[30] This issue was recently discussed by Zimmerman and Zucker.[31] Although we did not detect impairment of brain mitochondrial respiratory complexes in SHRSP, we propose that mitochondria-derived ROS mediate sympathoexcitation via NAD(P)H oxidase activation.[29]

Another possibility for ROS generation is uncoupling nitric oxide synthase (NOS). In the absence of L-arginine or with tetrahydrobiopterin, NO production from inducible NOS (iNOS) causes uncoupling from the oxidation of NADPH, resulting in superoxide generation.[9] iNOS overexpression in the RVLM causes hypertension and sympathoexcitation that is mediated by an increase in oxidative stress.[32] This might be relevant to our observation that iNOS expression levels in the RVLM are greater in SHRSP than in WKY rats.[33] In addition, microinjection of iNOS antagonists into the RVLM reduces blood pressure only in SHR, but not in WKY rats.[33]

ROS-Mediated Activation of Transcriptional Factors

It has been suggested that an Ang II-mediated influx of Ca^{2+} in neurons depends on increased superoxide generation by a Rac1-dependent NAD(P)H oxidase.[34] Ang II also regulates neuronal activity via inhibition of the delayed rectifier potassium current.[35] Ang II-mediated upregulation of L-type Ca^{2+} currents in neurons isolated from the NTS is inhibited by scavenging ROS, indicating a role for NAD(P)H oxidase-derived superoxide in the activation of Ca^{2+} channels in the NTS.[24]

NAD(P)H oxidase-derived superoxide mediates an Ang II-induced pressor effect via the activation of p38 mitogen-activated protein kinase (MAPK) in the RVLM.[36] Recently, we suggested that AT1 receptor-activated caspase-3 acting through the Ras/p38 MAPK/extracellular signal-related protein kinase pathway in the RVLM is involved in sympathoexcitation in SHRSP.[37] These pathways may be downstream effectors of ROS in the RVLM, which in turn plays a crucial role in the pathogenesis of hypertension. Interestingly, the pro-apoptotic proteins Bax and Bad were enhanced and the anti-apoptotic protein Bcl-2 was decreased in the RVLM of SHRSP, and inhibition of caspase-3 normalized these changes in pro- and anti-apoptotic protein levels.[37] These alterations in the RVLM of SHRSP were stimulated by Ang II via activation of the AT1 receptors, which are upregulated in this strain and other hypertensive models.[38] It would be reasonable to consider that different mechanisms may be responsible for sympathoexcitation in different brain sites (influx of Ca^{2+} for RVLM, apoptosis for NTS), and activation of the apoptotic pathway is involved in sympathoexcitation in the RVLM.[37] The exact physiologic implication of these observations requires further evaluation.

Effects of Angiotensin Receptor Blockers on Brain Oxidative Stress

The existence of an independent renin–angiotensin system in the brain is well established. Activation of the brain renin–angiotensin system substantially contributes to the development and maintenance of hypertension through activation of the sympathetic nervous system, vasopressin release, and drinking behavior.[39,40] There is considerable evidence that

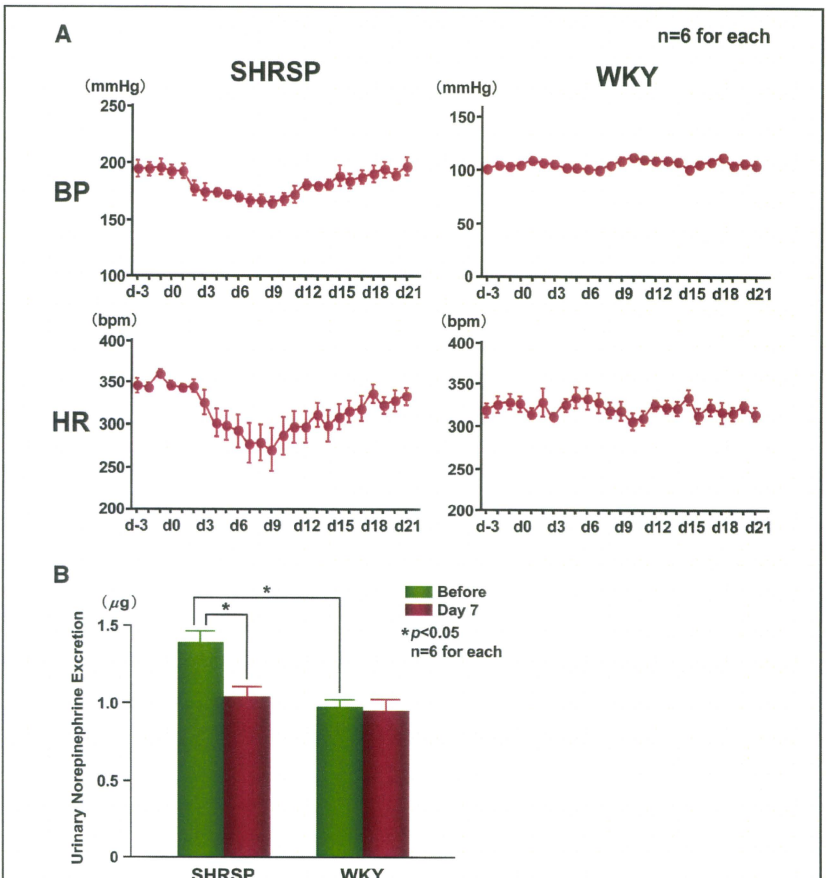

Figure 3. Inhibition of Rac1-dependent superoxide production in the rostral ventrolateral medulla (RVLM) decreases blood pressure, heart rate, and urinary norepinephrine excretion in stroke-prone spontaneously hypertensive rats (SHRSP). (**A**) Time course of mean blood pressure (BP) and heart rate (HR) before and after gene transfer of dominant negative Rac1 (DNRac1). (**B**) Twenty-four-hour urinary norepinephrine excretion before and after gene transfer of DNRac1 into the RVLM. d, day; WKY, Wistar–Kyoto rats.

peripherally administered angiotensin receptor blockers (ARBs) penetrate the blood–brain barrier, although there are some differences among ARBs.[41,42] AT1 receptors are abundant in the circumventricular organs, such as the subfornical organ and the organum vasculosum lamina terminalis, and the area postrema, which lack a blood–brain barrier.[39–42] Therefore, peripherally administered ARBs can also bind to those areas, thereby inhibiting the central actions of Ang II. Oral treatment with the ARB telmisartan appears to inhibit the central responses to Ang II in awake rats.[43] Although other ARBs also inhibit the central actions of Ang II within the brain beyond the blood–brain barrier,[41,42,44] these effects might differ depending on the pharmacokinetics and properties of each drug (ie, lipophilicity etc).[43] We evaluated the

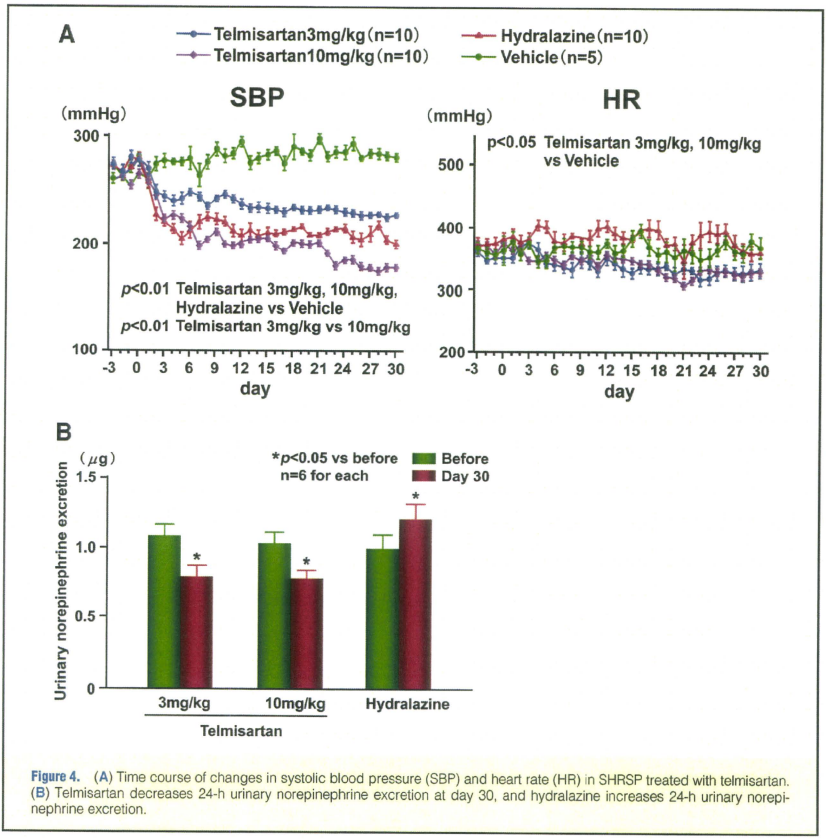

Figure 4. (A) Time course of changes in systolic blood pressure (SBP) and heart rate (HR) in SHRSP treated with telmisartan. (B) Telmisartan decreases 24-h urinary norepinephrine excretion at day 30, and hydralazine increases 24-h urinary norepinephrine excretion.

effect of treatment with telmisartan at either a high dose ($10\,mg \cdot kg^{-1} \cdot day^{-1}$) or a low dose ($3\,mg \cdot kg^{-1} \cdot day^{-1}$), or hydralazine for 30 days on hypertension.[45] Systolic blood pressure (SBP) and heart rate were measured using the tail-cuff method. Urinary norepinephrine excretion was measured as a marker of the sympathetic nervous system activity. We evaluated ROS in the brain (cortex, cerebellum, hypothalamus, and brainstem) of SHRSP on ESR spectroscopy and TBARS. Oral treatment with telmisartan reduced SBP dose-dependently and hydralazine reduced SBP to a similar level to the high dose of telmisartan (Figure 4). Telmisartan reduced, while hydralazine increased, urinary norepinephrine excretion (Figure 4). TBARS levels were significantly increased in each area of the brain of SHRSP compared with WKY rats (Figure 5). Oral treatment with telmisartan reduced the TBARS levels, but hydralazine did not (Figure 5). These findings suggest that (1) anti-hypertensive treatment with telmisartan reduces ROS in the brain of SHRSP; (2) telmisartan decreases blood pressure, at least in part, via a reduction of the sympathetic nervous system activity in SHRSP; and (3) these effects induced by telmisartan might be associated with protection of the brain of SHRSP from oxidative stress. We also measured the concentration of hydroxyl radicals using a modified procedure based on the hydroxylation of sodium salicylate by hydroxyl radicals,[46] leading to the production of 2,3-dihydroxybenzoic acid (2,3-DHBA).[29,47] Inhibition of Rac1 in the RVLM and oral treatment with telmisartan significantly decreased the production of hydroxyl radicals in the RVLM (Figure 6).[47]

Recently, we used in vivo ESR to assess oxidative stress in the brain, and found that oral treatment with another ARB, olmesartan, reduces oxidative stress in the brain of SHRSP without inducing reflex activation of the sympathetic nervous system.[48] In that study we evaluated the in vivo ESR signal

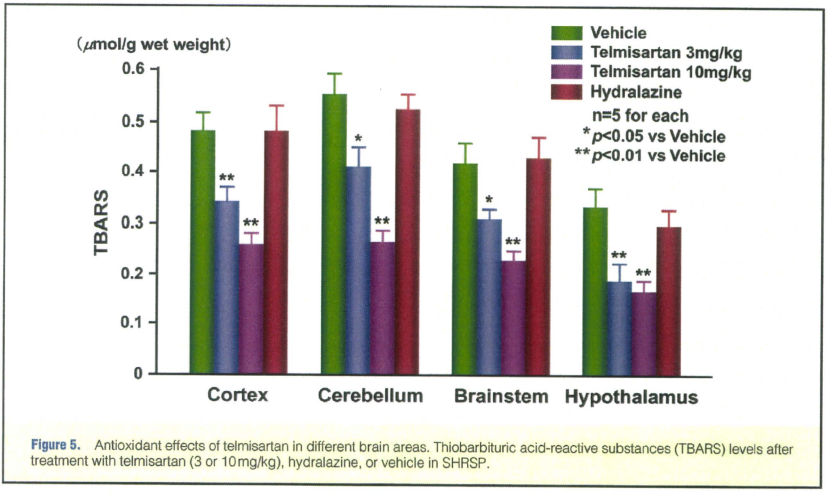

Figure 5. Antioxidant effects of telmisartan in different brain areas. Thiobarbituric acid-reactive substances (TBARS) levels after treatment with telmisartan (3 or 10mg/kg), hydralazine, or vehicle in SHRSP.

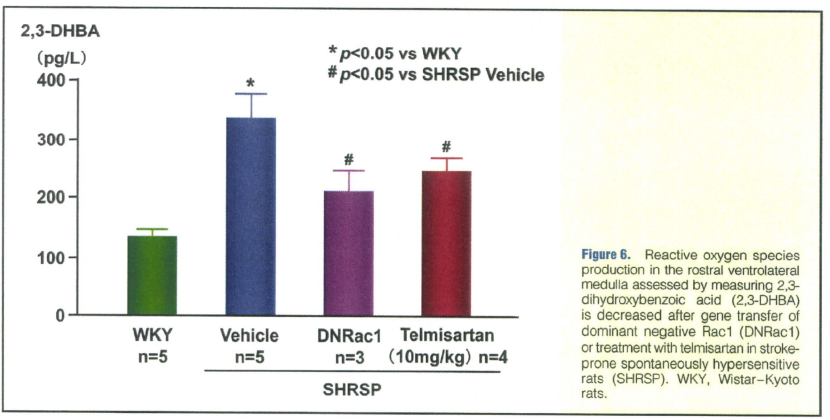

Figure 6. Reactive oxygen species production in the rostral ventrolateral medulla assessed by measuring 2,3-dihydroxybenzoic acid (2,3-DHBA) is decreased after gene transfer of dominant negative Rac1 (DNRac1) or treatment with telmisartan in stroke-prone spontaneously hypersensitive rats (SHRSP). WKY, Wistar–Kyoto rats.

decay rates of the brain using methoxycarbonyl-PROXYL, a nitroxyl radical species, as a blood–brain barrier-permeable spin probe.[49] Oral treatment with olmesartan attenuated the exaggerated pressor response to an excitatory amino acid, L-glutamate, in the RVLM of SHR compared to WKY rats.[50] Further, the pressor response to microinjection of Ang II into the RVLM was diminished in SHR treated with olmesartan.[50] Thus, the importance of oxidative stress in the brain and hypertension is supported by our studies as well as those of others.[11]

Several questions, however, remain to be answered. A recent study suggested that systemic administration of candesartan reduces brain Ang II levels because it attenuates the mRNA expression of both angiotensinogen and angiotensin-converting enzyme in Ang II-infused rats.[51] Whether systemic treatment with ARBs indirectly regulates brain Ang II remains to be determined.[52]

Effects of Other Cardiovascular Drugs on Brain Oxidative Stress

Considering that ARBs act to inhibit NAD(P)H oxidase activ-

ity, it is reasonable that ARBs have an antioxidant effect, although there are some unresolved questions, as mentioned previously. Calcium channel blockers, azelnidipine and amlodipine, but not nicardipine, which also have antioxidant properties, have a sympatho-inhibitory effect on the brain.[53,54] In particular, treatment with azelnidipine reduces oxidative stress in the RVLM associated with a decrease in the activity of NAD(P)H oxidase, Cu/Zn-SOD, and Mn-SOD.[53] These effects might be related to an improvement in NO production,[55] because we also demonstrated that overexpression of endothelial NOS in the NTS or RVLM decreases blood pressure and heart rate via the inhibition of sympathetic nervous system activity.[56–59] Surprisingly, we also found that atorvastatin inhibits the sympathetic nervous system as a result of upregulating NO activity and reducing oxidative stress.[60–63] Further studies are needed to determine if this mechanism is also applicable in humans.

Salt-Sensitive Hypertension and Brain Oxidative Stress

Activation of the sympathetic nervous system, in particular, an increase in central sympathetic outflow, plays an important role in the pathogenesis of salt-sensitive hypertension as well as that of kidney diseases.[64,65] Recent studies suggest that oxidative stress in the brain contributes to blood pressure elevation in salt-sensitive hypertension.[66,67] We demonstrated that high salt intake exacerbates blood pressure elevation and sympathetic nervous system activity during the development of hypertension in SHR, and these responses are mediated by increased ROS generation, probably because of an upregulation of AT1 receptors and NAD(P)H oxidase in the RVLM.[66] The findings of a recent study from Kyushu University Graduate School of Medical Sciences indicate that mice with pressure overload acquired brain salt-sensitivity.[68] This means that high salt intake increases the transport from the blood to the cerebrospinal fluid and the response of the sympathetic nerve activity to salt administered into the brain. These results suggest that pressure overload affects salt sensitivity, thereby enhancing central sympathetic outflow and cardiac function.[68] Left ventricular hypertrophy is an independent risk of cardiovascular event and high salt intake is an important environmental factor of hypertension, both of which increased ROS, and sympathoexcitation may be involved in the pathogenesis of the development of hypertension. A recent clinical trial suggested that left ventricular hypertrophy is related to cardiovascular events in Japanese high-risk hypertensive patients.[69]

Summary and Future Perspectives

Currently in Japan, many patients with hypertension also have metabolic syndrome. Importantly, the prevalence of metabolic syndrome increases linearly with an increase in heart rate among Japanese men and women,[70] suggesting that activation of the sympathetic nervous system is involved in the pathogenesis of hypertension.[71] The prevalence of obstructive sleep apnea has increased as a result of the increase in the number of obese patients with hypertension. Obese patients with sleep apnea have enhanced central sympathetic outflow, which worsens hypertension and leads to cardiovascular events.[72] Further, there is considerable evidence that psychological stress is a major risk factor for cardiovascular diseases and events associated with hypertension.[73] Another therapeutic target for the treatment of hypertension is heart failure with a preserved ejection fraction.[74] As suggested here, salt-sensitivity might also be enhanced in these patients, thereby further enhancing central sympathetic outflow.[68] Oxidative stress in the brain as well as other organs might underlie these mechanisms. Future studies of the effects of oxidative stress in the brain are warranted and will provide useful information for the treatment of hypertension.

Acknowledgments

We thank the many collaborators at Kyushu University Graduate School of Medical Sciences for their help and advice. We also thank Professor emeritus Akira Takeshita (deceased last March) for his continuing encouragement and support of this series of studies. This series of studies was supported by Grants-in-Aid for Scientific Research from Japan Society for the Promotion of Science.

References

1. Grassi G. Assessment of sympathetic cardiovascular drive in human hypertension: Achievements and perspectives. *Hypertension* 2009; **54:** 690–697.
2. Esler M. Pathophysiology of the human sympathetic nervous system in cardiovascular diseases: The transition from mechanisms to medical management. *J Appl Physiol* 2010; **108:** 227–237.
3. Guyenet PG. The sympathetic control of blood pressure. *Nat Rev Neurosci* 2006; **7:** 335–346.
4. Dampney RAL. Functional organization of central pathways regulating the cardiovascular system. *Physiol Rev* 1994; **74:** 323–364.
5. Pilowsky PM, Goodchild AK. Baroreceptor reflex pathways and neurotransmitters: 10 years on. *J Hypertens* 2002; **20:** 1675–1688.
6. Sved AF, Ito S, Sved JC. Brainstem mechanisms of hypertension: Role of the rostral ventrolateral medulla. *Curr Hypertens Rep* 2003; **5:** 262–268.
7. Campos RR, Bergamaschi CT. Neurotransmission alterations in central cardiovascular control in experimental hypertension. *Curr Hypertens Rev* 2006; **2:** 193–198.
8. Paravicini T, Touyz RM. Redox signaling in hypertension. *Cardiovasc Res* 2006; **71:** 247–258.
9. Hirooka Y. Role of reactive oxygen species in brainstem in neural mechanisms of hypertension. *Auton Neurosci* 2008; **142:** 20–24.
10. Peterson JR, Sharma RV, Davisson RL. Reactive oxygen species in the neuropathogenesis of hypertension. *Curr Hypertens Rep* 2006; **8:** 232–241.
11. Campos RR. Oxidative stress in the brain and arterial hypertension. *Hypertens Res* 2009; **32:** 1047–1048.
12. Zimmerman MC, Lazartigues E, Lang JA, Sinnayah P, Ahmad IM, Spitz DR, et al. Superoxide mediates the action of angiotensin II in the central nervous system. *Circ Res* 2002; **91:** 1038–1045.
13. Zimmerman MC, Lazartigues E, Sharma RV, Davisson RL. Hypertension caused by angiotensin II infusion involves increased superoxide production in the central nervous system. *Circ Res* 2004; **95:** 210–216.
14. Kishi T, Hirooka Y, Kimura Y, Ito K, Shimokawa H, Takeshita A. Increased reactive oxygen species in rostral ventrolateral medulla contribute to neural mechanisms of hypertension in stroke-prone spontaneously hypertensive rats. *Circulation* 2004; **109:** 2357–2362.
15. Ohtsuki T, Matsumoto M, Suzuki K, Taniguchi N, Kamada T. Mitochondrial lipid peroxidation and superoxide dismutase in rat hypertensive target organs. *Am J Physiol Heart Circ Physiol* 1995; **268:** H1418–H1421.
16. Kimoto-Kinoshita S, Nishida S, Tomura TT. Age-related change of antioxidant capacities in the cerebral cortex and hippocampus of stroke-prone spontaneously hypertensive rats. *Neurosci Lett* 1999; **273:** 41–44.
17. Rikans LE, Hornbrook KR. Lipid peroxidation, antioxidant protection and aging. *Biochim Biophys Acta* 1997; **1362:** 116–127.
18. Sano H, Matsumoto K, Utsumi H. Synthesis and imaging of blood-brain-barrier permeable nitroxyl-probes for free radical reactions in brain of living mice. *Biochem Mol Biol Int* 1997; **42:** 641–647.
19. Tai MH, Wang LL, Wu KL, Chan JY. Increased superoxide anion in rostral ventrolateral medulla contributes to hypertension in spontaneously hypertensive rats via interactions with nitric oxide. *Free Radic Biol Med* 2005; **38:** 450–462.
20. Chan SHH, Tai MH, Li CY, Chan JYH. Reduction in molecular synthesis or enzyme activity of superoxide dismutase and catalase contributes to oxidative stress and neurogenic hypertension in spon-

taneously hypertensive rats. *Free Radic Biol Med* 2006; **40:** 2028–2039.
21. Oliveira-Sales EB, Dugaich AP, Carillo BA, Abreu NP, Boim MA, Martins PJ, et al. Oxidative stress contributes to renovascular hypertension. *Am J Hypertens* 2008; **21:** 98–104.
22. Oliveira-Sales EB, Nishi EE, Carillo BA, Boim MA, Dolnikoff MS, Bergamaschi CT, et al. Oxidative stress in the sympathetic premotor neurons contributes to sympathetic activation in renovascular hypertension. *Am J Hypertens* 2009; **22:** 484–492.
23. Lassegue B, Clempus RE. Vascular NAD(P)H oxidases: Specific features, expression, and regulation. *Am J Physiol Regul Integr Comp Physiol* 2003; **285:** R277–R297.
24. Wang G, Anrather J, Huang J, Speth RC, Pickel VM, Iadecola C. NADPH oxidase contributes angiotensin signaling in the nucleus tractus solitarius. *J Neurosci* 2004; **24:** 5516–5524.
25. Wang G, Anrather J, Glass MJ, Tarsitano J, Zhou P, Frys KA, et al. Nox2, Ca^{2+}, and protein kinase C play a role in angiotensin II-induced free radical production in nucleus tractus solitarius. *Hypertension* 2006; **48:** 482–489.
26. Zimmerman MC, Dunlay RP, Larzartigues E, Zhang Y, Sharma RV, Engelhardt JF, et al. Requirement for Rac1-dependent NADPH oxidase in the cardiovascular and dipsogenic actions of angiotensin II in the brain. *Circ Res* 2004; **95:** 532–539.
27. Sagara Y, Hirooka Y, Kimura Y, Nozoe M, Sunagawa K. Increased reactive oxygen species via Rac1-dependent pathway in rostral ventrolateral medulla contribute to neural mechanisms of hypertension in stroke-prone spontaneously hypertensive rats. *Circulation* 2005; **112**(Suppl II): II-154.
28. Nozoe M, Hirooka Y, Koga Y, Sagara Y, Kishi T, Engelhardt JF, et al. Inhibition of Rac1-derived reactive oxygen species in nucleus tractus solitarius decreases blood pressure and heart rate in stroke-prone spontaneously hypertensive rats. *Hypertension* 2007; **50:** 62–68.
29. Nozoe M, Hirooka Y, Koga Y, Araki S, Konno S, Kishi T, et al. Mitochondria-derived reactive oxygen species mediate sympathoexcitation induced by angiotensin II in the rostral ventrolateral medulla. *J Hypertens* 2008; **26:** 2176–2184.
30. Chan SHH, Wu KLH, Chang AYW, Tai MH, Chan JYH. Oxidative impairment of mitochondrial electron transport chain complexes in rostral ventrolateral medulla contributes to neurogenic hypertension. *Hypertension* 2009; **53:** 217–227.
31. Zimmerman MC, Zucker IH. Mitochondrial dysfunction and mitochondrial-produced reactive oxygen species: New targets for neurogenic hypertension? *Hypertension* 2009; **53:** 112–114.
32. Kimura Y, Hirooka Y, Sagara Y, Ito K, Kishi T, Shimokawa H, et al. Overexpression of inducible nitric oxide synthase in rostral ventrolateral medulla causes hypertension and sympathoexcitation via an increase in oxidative stress. *Circ Res* 2005; **96:** 252–260.
33. Kimura Y, Hirooka Y, Kishi T, Ito K, Sagara Y, Sunagawa K. Role of inducible nitric oxide synthase in rostral ventrolateral medulla in blood pressure regulation in spontaneously hypertensive rats. *Clin Exp Hypertens* 2009; **31:** 281–286.
34. Zimmerman MC, Sharma RV, Davisson RL. Superoxide mediates angiotensin II-induced influx of extracellular calcium in neural cells. *Hypertension* 2005; **45:** 717–723.
35. Sun C, Sellers KW, Sumners C, Raizada MK. NAD(P)H oxidase inhibition attenuates neuronal chronotropic actions of angiotensin II. *Circ Res* 2005; **96:** 659–666.
36. Chan SHH, Hsu KS, Hunag CC, Wang LL, Ou CC, Chan JYH. NADPH oxidase-derived superoxide anion mediates angiotensin II-induced pressor effect via activation of p38 mitogen-activated protein kinase in the rostral ventrolateral medulla. *Circ Res* 2005; **97:** 772–780.
37. Kishi T, Hirooka Y, Konno S, Ogawa K, Sunagawa K. Angiotensin II type 1 receptor-activated caspase-3 through Ras/mitogen-activated protein kinase/extracellular signal-regulated kinase in the rostral ventrolateral medulla is involved in sympathoexcitation in stroke-prone spontaneously hypertensive rats. *Hypertension* 2010; **55:** 291–297.
38. Reja V, Goodchild AK, Phillips JK, Pilowsky PM. Upregulation of angiotensin AT_1 receptor and intracellular kinase gene expression in hypertensive rats. *Clin Exp Pharmacol Physiol* 2006; **33:** 690–695.
39. McKinley MJ, Albiston AL, Allen AM, Mathai M, May CN, McAllen RM, et al. The brain renin-angiotensin system: Location and physiological roles. *Int J Biochem Cell Biol* 2003; **35:** 901–918.
40. Dampney RAL, Fontes MAP, Hirooka Y, Potts PD, Tagawa T. Role of angiotensin II receptors in the regulation of vasomotor neurons in the rostral ventrolateral medulla. *Clin Exp Pharmacol Physiol* 2002; **29:** 467–472.
41. Wang JM, Tan J, Leenen FHH. Central nervous system blockade by peripheral administration of AT_1 receptor blockers. *J Cardiovasc Pharmacol* 2003; **41:** 593–599.
42. Culman J, Blume A, Gohlke P, Unger T. The renin-angiotensin system in the brain: Possible therapeutic implications for AT_1-receptor blockers. *J Hum Hypertens* 2002; **16:** S64–S70.
43. Gohlke P, Weiss S, Jansen A, Wienen W, Stangier J, Rascher W, et al. AT_1 receptor antagonist telemisartan administered peripherally inhibits central responses to angiotensin II in conscious rats. *J Pharmacol Exp Ther* 2001; **298:** 62–70.
44. Nishimura Y, Ito T, Hoe KL, Saavedra JM. Chronic peripheral administration of the angiotensin II AT_1 receptor antagonist candesartan blocks brain AT_1 receptors. *Brain Res* 2000; **871:** 29–38.
45. Sagara Y, Ito K, Kimura Y, Hirooka Y. Telmisartan reduces oxidative stress in the brain with sympathoinhibitory effects in stroke-prone spontaneously hypertensive rats. *Circulation* 2004; **110**(Suppl III): 265.
46. Yang CY, Lin MT. Oxidative stress in rats with heatstroke-induced cerebral ischemia. *Stroke* 2002; **33:** 790–794.
47. Sagara Y, Hirooka Y, Nozoe M, Koga Y, Sunagawa K. Contribution of angiotensin II in the increased reactive oxygen species in rostral ventrolateral medulla and enhanced central sympathetic outflow in stroke-prone spontaneously hypertensive rats. *Circulation* 2006; **114**(Suppl II): 271.
48. Araki S, Hirooka Y, Kishi T, Yasukawa K, Utsumi H, Sunagawa K. Olmesartan reduces oxidative stress in the brain of stroke-prone spontaneously hypertensive rats assessed by an in vivo ESR method. *Hypertens Res* 2009; **32:** 1091–1096.
49. Sano H, Naruse M, Matsumoto K, Oi T, Utsumi H. A new nitroxyl-probe with high retention in the brain and its application for brain imaging. *Free Radic Biol Med* 2000; **28:** 959–969.
50. Lin Y, Matsumura K, Kagiyama S, Fukuhara M, Fujii K, Iida M. Chronic administration of olmesartan attenuates the exaggerated pressor response to glutamate in the rostral ventrolateral medulla of SHR. *Brain Res* 2005; **1058:** 161–166.
51. Pelisch N, Hosomi N, Ueno M, Masugata H, Murao K, Hitomi H, et al. Systemic candesartan reduces brain angiotensin II via down-regulation of brain renin-angiotensin system. *Hypertens Res* 2010; **33:** 161–164.
52. Mogi M, Horiuchi M. Remote control of brain angiotensin II levels by angiotensin receptor blockers. *Hypertens Res* 2010; **33:** 116–117.
53. Konno S, Hirooka Y, Araki S, Koga Y, Kishi T, Sunagawa K. Azelnidipine decreases sympathetic nerve activity via antioxidant effect in the rostral ventrolateral medulla of stroke-prone spontaneously hypertensive rats. *J Cardiovasc Pharmacol* 2008; **52:** 555–560.
54. Hirooka Y, Kimura Y, Nozoe M, Sagara Y, Ito K, Sunagawa K. Amlodipine-induced reduction of oxidative stress in the brain is associated with sympatho-inhibitory effects in stroke-prone spontaneously hypertensive rats. *Hypertens Res* 2006; **29:** 49–56.
55. Kimura Y, Hirooka Y, Sagara Y, Sunagawa K. Long-acting calcium channel blocker, azelnidipine, increases endothelial nitric oxide synthase in the brain and inhibits sympathetic nerve activity. *Clin Exp Hypertens* 2007; **29:** 13–21.
56. Sakai K, Hirooka Y, Matsuo I, Eshima K, Shigematsu H, Shimokawa H, et al. Overexpression of eNOS in NTS causes hypotension and bradycardia in vivo. *Hypertension* 2000; **36:** 1023–1028.
57. Kishi T, Hirooka Y, Sakai K, Shigematsu H, Shimokawa H, Takeshita A. Overexpression of eNOS in the RVLM causes hypotension and bradycardia via GABA release. *Hypertension* 2001; **38:** 896–901.
58. Kishi T, Hirooka Y, Ito K, Sakai K, Shimokawa H, Takeshita A. Cardiovascular effects of endothelial nitric oxide synthase in the rostral ventrolateral medulla in stroke-prone spontaneously hypertensive rats. *Hypertension* 2002; **39:** 264–268.
59. Kishi T, Hirooka Y, Kimura Y, Sakai K, Ito K, Shimokawa H, et al. Overexpression of eNOS in RVLM improves impaired baroreflex control of heart rate in SHRSP. *Hypertension* 2003; **41:** 255–260.
60. Kishi T, Hirooka Y, Shimokawa H, Takeshita A, Sunagawa K. Atorvastatin reduces oxidative stress in the rostral ventrolateral medulla of stroke-prone spontaneously hypertensive rats. *Clin Exp Hypertens* 2008; **30:** 1–9.
61. Kishi T, Hirooka Y, Konno S, Sunagawa K. Sympathoinhibition induced by centrally administered atorvastatin is associated with alteration of NAD(P)H and Mn superoxide dismutase activity in rostral ventrolateral medulla of stoke-prone spontaneously hyper-

tensive rats. *J Cardiovasc Pharmacol* 2010; **55:** 184–190.
62. Kishi T, Hirooka Y, Konno S, Sunagawa K. Atorvastatin improves the impaired baroreflex sensitivity via anti-oxidant effect in the rostral ventrolateral medulla of SHRSP. *Clin Exp Hypertens* 2009; **31:** 698–704.
63. Kishi T, Hirooka Y, Mukai Y, Shimokawa H, Takeshita A. Atorvastatin causes depressor and sympatho-inhibitory effects with upregulation of nitric oxide synthase in stroke-prone spontaneously hypertensive rats. *J Hypertens* 2003; **21:** 379–386.
64. Huang BS, Amin S, Leenen FHH. The central role of the brain in salt-sensitive hypertension. *Curr Opin Cardiol* 2006; **21:** 295–304.
65. Brooks VL, Haywood JR, Johnson AK. Translation of salt retention to central activation of the sympathetic nervous system in hypertension. *Clin Exp Pharmacol Physiol* 2005; **32:** 426–432.
66. Koga Y, Hirooka Y, Araki S, Nozoe M, Kishi T, Sunagawa K. High salt intake enhances blood pressure increase during development of hypertension via oxidative stress in rostral ventrolateral medulla of spontaneously hypertensive rats. *Hypertens Res* 2008; **31:** 2075–2083.
67. Fujita M, Ando K, Nagase A, Fujita T. Sympathoexcitation by oxidative stress in the brain mediates arterial pressure elevation in salt-sensitive hypertension. *Hypertension* 2007; **50:** 360–367.
68. Ito K, Hirooka Y, Sunagawa K. Acquisition of brain Na sensitivity contributes to salt-induced sympathoexcitation and cardiac dysfunction in mice with pressure overload. *Circ Res* 2009; **104:** 1004–1011.
69. Ueshima K, Yasuno S, Oba K, Fujimoto A, Ogihara T, Saruta T, et al. Effects of cardiac complications on cardiovascular events in Japanese high-risk hypertensive patients: Subanalysis of the CASE-J Trial. *Circ J* 2009; **73:** 1080–1085.
70. Oda E, Kawai R. Significance of heart rate in the prevalence of metabolic syndrome and its related risk factors in Japanese. *Circ J* 2009; **73:** 1431–1436.
71. Mancia G, Bousquet P, Elghozi JL, Esler M, Grassi G, Julius S, et al. The sympathetic nervous system and the metabolic syndrome. *J Hypertens* 2007; **25:** 909–920.
72. Kato M, Adachi T, Koshino Y, Somers VK. Obstructive sleep apnea and cardiovascular disease. *Circ J* 2009; **73:** 1363–1370.
73. Hata S. Cardiovascular disease caused by earthquake-induced stress: Psychological stress and cardiovascular disease. *Circ J* 2009; **73:** 1195–1196.
74. Yamamoto K, Sakata Y, Ohtani T, Takeda Y, Mano T. Heart failure with preserved ejection fraction: What is known and unknown. *Circ J* 2009; **73:** 404–410.

Angiotensin II Type 1 Receptor–Activated Caspase-3 Through Ras/Mitogen-Activated Protein Kinase/Extracellular Signal-Regulated Kinase in the Rostral Ventrolateral Medulla Is Involved in Sympathoexcitation in Stroke-Prone Spontaneously Hypertensive Rats

Takuya Kishi, Yoshitaka Hirooka, Satomi Konno, Kiyohiro Ogawa, Kenji Sunagawa

Abstract—In the rostral ventrolateral medulla (RVLM), angiotensin II-derived superoxide anions, which increase sympathetic nerve activity, induce a pressor response by activating the p38 mitogen-activated protein kinase (p38 MAPK) and extracellular signal-regulated kinase (ERK) pathway. The small G protein Ras mediates a caspase-3–dependent apoptotic pathway through p38 MAPK, ERK, and c-Jun N-terminal kinase. We hypothesized that angiotensin II type 1 receptors activate caspase-3 through the Ras/p38 MAPK/ERK/c-Jun N-terminal kinase pathway in the RVLM and that this pathway is involved in sympathoexcitation in stroke-prone spontaneously hypertensive rats (SHRSP), a model of human hypertension. The activities of Ras, p38 MAPK, ERK, and caspase-3 in the RVLM were significantly higher in SHRSP (14 to 16 weeks old) than in age-matched Wistar-Kyoto rats (WKY). The mitochondrial apoptotic proteins Bax and Bad in the RVLM were significantly increased in SHRSP compared with WKY. c-Jun N-terminal kinase activity did not differ between SHRSP and WKY. In SHRSP, intracerebroventricular infusion of a Ras inhibitor significantly reduced sympathetic nerve activity and improved baroreflex sensitivity, partially because of inhibition of the Ras/p38 MAPK/ERK, Bax, Bad, and caspase-3 pathway in the RVLM. Intracerebroventricular infusion of a caspase-3 inhibitor also inhibited sympathetic nerve activity and improved baroreflex sensitivity in SHRSP. Intracerebroventricular infusion of an angiotensin II type 1 receptor blocker in SHRSP partially inhibited the Ras/p38 MAPK/ERK, Bax, Bad, and caspase-3 pathway in the RVLM. These findings suggest that in SHRSP, angiotensin II type 1 receptor-activated caspase-3 acting through the Ras/p38 MAPK/ERK pathway in the RVLM might be involved in sympathoexcitation, which in turn plays a crucial role in the pathogenesis of hypertension. (***Hypertension*. 2010;55:291-297.**)

Key Words: angiotensin II ■ apoptosis ■ sympathetic nerve activity ■ brain ■ hypertension

Neuronal apoptosis in the brain is involved in regulating synaptic plasticity and neural function[1–3] and is mainly caused by reactive oxygen species (ROS).[4–8] Ras is a member of a superfamily of related small GTPases implicated in cellular proliferation and transformation, growth arrest, senescence, and apoptosis.[9–13] In cultured tumor cells or endothelial cells, the proapoptotic effects of Ras are mediated by the p38 mitogen-activated protein kinase (MAPK) and extracellular signal-regulated kinase (ERK) pathway through phosphorylation of the proapoptotic proteins Bax and Bad and the antiapoptotic protein Bcl-2, which releases cytochrome *c* in the mitochondria.[14–17] Neuronal apoptosis is characterized by the release of cytochrome *c*, which activates caspase-3, the major executioner caspase in neurons.[18,19] Thus, neuronal apoptosis may be mainly mediated by caspase-3 through the Ras, p38 MAPK, ERK pathway. We previously demonstrated that ROS in a cardiovascular center of the brain stem increase sympathetic nerve activity (SNA) in hypertensive rats.[20] Accumulating evidence suggests that ROS in the brain are involved in the neural mechanisms of hypertension.[21,22] Although ROS are increased in the brain in a hypertensive state, it is not known whether a pivotal signaling pathway (such as the Ras, p38 MAPK, ERK pathway) and caspase-3, activated by ROS in the brain, are chronically activated in the hypertensive state or whether this pathway activates SNA.

The rostral ventrolateral medulla (RVLM) in the brain stem is a major vasomotor center, and it regulates SNA.[23,24] We previously demonstrated that ROS in the RVLM activates SNA and that ROS are increased in the RVLM of stroke-prone spontaneously hypertensive rats (SHRSP), a model of human hypertension,[25] with activation of SNA.[20] In the brain, ROS are produced by activation of the angiotensin II type 1 receptor (AT_1R), which in turn activates nicotinamide-

Received June 30, 2009; first decision July 20, 2009; revision accepted December 7, 2009.

From the Department of Cardiovascular Medicine, Kyushu University Graduate School of Medical Sciences, Fukuoka, Japan.

Correspondence to Yoshitaka Hirooka, Department of Cardiovascular Medicine, Kyushu University Graduate School of Medical Sciences, 3-1-1 Maidashi, Higashi-ku, Fukuoka 812-8582, Japan. E-mail hyoshi@cardiol.med.kyushu-u.ac.jp

Hypertension **is available at http://hyper.ahajournals.org** **DOI: 10.1161/HYPERTENSIONAHA.109.138636**

adenine dinucleotide phosphate (NAD[P]H) oxidase.[26] NAD(P)H oxidase-derived superoxide anions mediate the angiotensin II-induced pressor effect via the activation of p38 MAPK and ERK in the RVLM.[27] Furthermore, in experimental endotoxemia, the proapoptotic protein Bax and caspase-3–dependent apoptosis in the RVLM mediate cardiovascular responses.[28] The mechanisms by which ROS in the RVLM regulate SNA have not been fully examined, especially the pivotal signaling pathway of ROS.

The aims of the present study were to determine whether stimulation of endogenous AT_1R activates caspase-3 through the Ras/p38 MAPK/ERK/c-Jun N-terminal kinase (JNK) pathway in the RVLM and, if so, to determine whether activation of this pathway is involved in the increased sympathoexcitation in SHRSP. Toward this end, we examined the activity of Ras, p38 MAPK, ERK, JNK, proapoptotic proteins Bax and Bad, antiapoptotic protein Bcl-2, and caspase-3 in the RVLM of SHRSP and normotensive rats. In addition, we performed intracerebroventricular (ICV) injections of a Ras inhibitor, a caspase-3 inhibitor, and an angiotensin receptor blocker (ARB), and examined the changes in blood pressure, heart rate (HR), SNA, and baroreflex sensitivity (BRS). To determine whether ICV injection of a Ras inhibitor, a caspase-3 inhibitor, or an ARB inhibits the pivotal signaling pathway in the RVLM, we also examined the changes in blood pressure, HR, and SNA evoked by microinjection of angiotensin II into the RVLM.

Methods

This study was reviewed and approved by the Committee on the Ethics of Animal Experiments at the Kyushu University Graduate School of Medical Sciences and conducted according to the Guidelines for Animal Experiments of Kyushu University. Details of the methods are available in the online Data Supplement at http://hyper.ahajournals.org.

Animals and General Procedures

Male SHRSP/Izm rats and age-matched Wistar-Kyoto rats (WKY) (14 to 16 weeks old), fed standard feed, were divided into 7 groups (SHRSP treated with Ras inhibitor [S-RI], SHRSP treated with caspase-3 inhibitor [S-CI], SHRSP treated with ARB [S-ARB], SHRSP treated with vehicle [S-Veh], WKY treated with Ras inhibitor [W-RI], WKY treated with caspase-3 inhibitor [W-CI], and WKY with vehicle [W-Veh]; n=5/group). In the S-RI, W-RI, S-CI, W-CI, S-Veh, W-Veh, and S-ARB groups, we measured blood pressure and HR using a radiotelemetry system as described previously.[20] Urinary norepinephrine excretion (uNE) for 24 hours was calculated as an indicator of SNA, as described previously.[20,22] Furthermore, in the S-RI, W-RI, S-CI, W-CI, S-Veh, and W-Veh groups, spectral analysis was performed to provide power spectra for systolic blood pressure.

Activity of Ras, p38 MAPK, ERK, JNK, and Caspase-3 and Expression of Bax, Bad, and Bcl-2 in the RVLM

The activity of Ras, p38 MAPK, ERK, JNK, and caspase-3 and the expression of Bax, Bad, and Bcl-2 in the RVLM were measured as described previously.[29]

ICV Injection of Ras Inhibitor, Caspase-3 Inhibitor, and AT_1R Blocker

S-Farnesylthiosalicylic acid (1 mmol/L), a specific Ras inhibitor[30]; *N*-benzyloxycarbonyl-Asp(OMe)-Glu(OMe)-Val-Asp(OMe) fluoromethyl ketone (Z-DEVD-FMK, 1 μmol/L), a specific caspase-3 inhibitor[31]; candesartan (1 μg/μL); or vehicle was administered by ICV infusion for 14 days with an osmotic minipump (Alzet 1003D). We also determined the changes in blood pressure and HR of SHRSP after terminating the 14-day ICV infusion of the Ras inhibitor (n=4). The candesartan dose was selected as described previously.[32]

Statistical Analysis

Normally distributed variables are expressed as mean±SE. Unpaired *t* and Mann-Whitney U tests were used to compare the differences in normally distributed and nonnormally distributed variables, respectively. Data were also analyzed by a 2-factor repeated-measures analysis of variances. Differences were considered to be statistically significant at $P<0.05$.

Results

Blood Pressure, HR, SNA, and BRS

The Ras inhibitor *S*-farnesylthiosalicylic acid was infused ICV for 14 days. Mean blood pressure (MBP), HR, uNE, and normalized unit of the low-frequency component of systolic blood pressure (LFnuSBP) at day 14 were significantly higher in S-Veh than in W-Veh (Figure 1A through 1D). MBP, HR, and LFnuSBP in SHRSP returned to control levels 4 days after terminating the ICV infusion of *S*-farnesylthiosalicylic acid (data not shown). BRS at day 14 was significantly lower in S-Veh than in W-Veh (Figure 2). At days 2 to 14, MBP and HR were significantly lower in S-RI than in S-Veh (Figure 1A and 1B), and at day 14, uNE and LFnuSBP were significantly lower in S-RI than in S-Veh (Figure 1C and 1D). BRS at day 14 was significantly higher in S-RI than in S-Veh (Figure 2). MBP, HR, LFnuSBP, uNE, and BRS, however, did not differ between W-RI and W-Veh (Figures 1A through 1D and 2).

The caspase-3 inhibitor Z-DEVD-FMK was infused ICV for 14 days. At days 4 to 14, MBP and HR were significantly lower in S-CI than in S-Veh (Figure 1A and 1B), and at day 14, uNE and LFnuSBP were also significantly lower in S-CI than in S-Veh (Figure 1C and 1D). BRS at day 14 was significantly higher in S-CI than in S-Veh (Figure 2). MBP, HR, LFnuSBP, uNE, and BRS did not differ between W-CI and W-Veh (Figures 1A through 1D and 2).

On day 14 of the ICV infusion of candesartan in SHRSP, the systolic blood pressure, HR, uNE, and LFnuSBP were significantly lower in S-ARB than in S-Veh (Figures 1A through 1D).

Ras, p38 MAPK, ERK, and JNK Activity in the RVLM

Ras, p38 MAPK, and ERK activities were significantly higher in S-Veh than in W-Veh and significantly lower in S-RI than in S-Veh (Figure 3A through 3C). Furthermore, Ras, p38 MAPK, and ERK activity was significantly lower in S-ARB than in S-Veh (Figure 3A through 3C). Ras, p38 MAPK, and ERK activity in SHRSP did not differ between S-CI and S-Veh (Figure 3A through 3C) or between W-Veh and W-CI (Figure 3A through 3C). JNK activity did not differ between S-Veh and W-Veh (Figure 3D).

Caspase-3 Activity and Expression of Bax, Bad, and Bcl-2 in the RVLM

Caspase-3 activity in the cytosolic fraction of the RVLM and the expression of Bax and Bad in the mitochondrial fraction of the RVLM were significantly higher in S-Veh than in W-Veh (Figure 4A through 4C) and significantly lower in

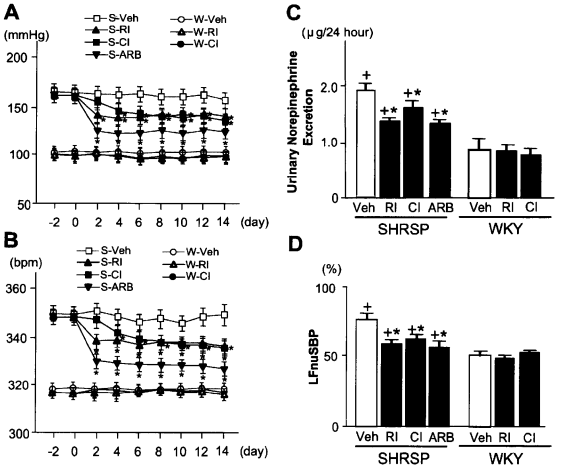

Figure 1. Time course of MBP (A, mm Hg) and HR (B, bpm) in S-RI (n=5), S-CI (n=5), S-ARB (n=5), S-Veh (n=5), W-RI (n=5), W-CI (n=5), and W-Veh (n=5). *P<0.05 for Ras inhibitor (RI), caspase-3 inhibitor (CI), or ARB vs vehicle (Veh) values in each strain. C and D, 24-hour uNE (μg) (C) and LFnuSBP (%) (D) on day 14 in SHRSP treated with RI, caspase-3 inhibitor (CI), ARB, or vehicle (Veh) and WKY treated with RI, caspase-3 inhibitor (CI), or Veh (n=5 for each). *P<0.05 for RI, CI, or ARB vs Veh values in each strain. +P<0.05 vs W-Veh. Data are shown as mean±SEM.

S-RI than in S-Veh (Figure 4A through 4C). ICV infusion of Z-DEVD-FMK significantly inhibited caspase-3 activity in both SHRSP and WKY (Figure 4A). In WKY, however, neither caspase-3 activity nor the expression of Bax and Bad differed between W-Veh and W-RI (Figure 4A through 4C). ICV infusion of candesartan in SHRSP significantly decreased caspase-3 activity and the expression of Bax and Bad (Figure 4A through 4C).

The expression of Bcl-2 was significantly lower in S-Veh than in W-Veh (Figure 4D) and significantly higher in S-RI than in S-Veh (Figure 4D). In WKY, however, the expression of Bcl-2 did not differ between W-Veh and W-RI (Figure 4D). ICV infusion of candesartan in SHRSP significantly increased Bcl-2 expression (Figure 4D).

Microinjection of Angiotensin II into the RVLM

The changes in MBP, HR, and LFnuSBP evoked by microinjection of angiotensin II into the bilateral RVLM were significantly smaller in S-RI than in S-Veh (MBP, 8±5 mm Hg versus 14±3 mm Hg; HR, 7±8 bpm versus 22±9 bpm; LFnuSBP, 3±3% versus 8±2%; n=5 for each; P<0.01).

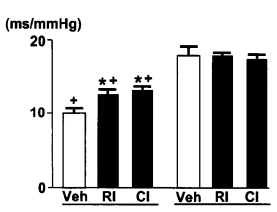

Figure 2. BRS (ms/mm Hg) in SHRSP and WKY treated with vehicle (Veh), Ras inhibitor (RI), or caspase-3 inhibitor (CI) (n=5 for each). *P<0.05 vs Veh in each strain. +P<0.05 vs W-Veh. Data are shown as mean±SEM.

Discussion

The novel findings in the present study are as follows: (1) Ras, p38 MAPK, ERK, mitochondrial apoptotic proteins Bax and Bad, and caspase-3 in the RVLM are activated in SHRSP; (2) ICV infusion of a Ras inhibitor decreases MBP, HR, and SNA and increases BRS through the partial inhibition of p38 MAPK, ERK, Bax, Bad, and caspase-3 in the RVLM of SHRSP; (3) ICV infusion of a caspase-3 inhibitor decreases MBP, HR, and SNA and increases BRS through the partial inhibition of caspase-3 in the RVLM of SHRSP; (4) ICV infusion of candesartan decreases systolic blood pressure, HR, and SNA through the partial inhibition of Ras, p38 MAPK, ERK, Bax, Bad, and caspase-3 in the RVLM of SHRSP; and (5) ICV infusion of the Ras inhibitor in SHRSP abolishes the pressor effect evoked by the microinjection of angiotensin II into the RVLM. These findings indicate that AT_1R-induced activation of caspase-3 through the Ras/p38 MAPK/ERK pathway in the RVLM might increase MBP, HR, and SNA and decrease BRS (Figure 5).

The present findings are the first to demonstrate that Ras, p38 MAPK, and ERK activity is increased in the RVLM of SHRSP. A previous study suggested that an acute injection of angiotensin II induced AT_1R-dependent ROS production and phosphorylation of p38 MAPK and ERK in the RVLM.[27] Activation of p38 MAPK and ERK by angiotensin II is also reported in mesenteric smooth muscle cells[33,34] and aorta.[35,36] In the forebrain, MAPK is activated in a model of heart failure in which the brain renin-angiotensin system is upregulated.[37] ROS activates Ras,[38] and Ras activates caspase-3 through p38 MAPK and ERK.[4-7,39] Previously, we demon-

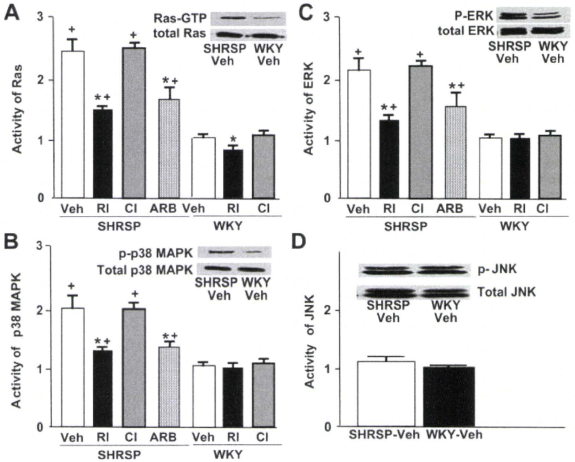

Figure 3. Activity of Ras (A), p38 MAPK (B), ERK (C), and JNK (D) in the RVLM on day 14 in SHRSP and WKY treated with vehicle (Veh), Ras inhibitor (RI), caspase-3 inhibitor (CI), or ARB (n=5/group). *$P<0.05$ vs Veh in each strain. +$P<0.05$ vs Veh-treated WKY. Activity is expressed relative to that in Veh-treated WKY, which was assigned a value of 1. Data are shown as mean±SEM.

strated that ROS in the RVLM increases SNA,[20,22] and ROS is produced in the brain by angiotensin II and NAD(P)H oxidase.[25] In the present study, ICV infusion of the Ras inhibitor decreased MBP, HR, and SNA and increased BRS because of the partial inhibition of Ras, p38 MAPK, ERK, and caspase-3 in the RVLM of SHRSP, and it abolished the pressor effect evoked by the microinjection of angiotensin II into the RVLM. ICV infusion of the caspase-3 inhibitor also inhibited MBP, HR, and SNA and increased BRS through the partial inhibition of caspase-3 activity in the RVLM of SHRSP. Furthermore, ICV infusion of candesartan decreased MBP, HR, and SNA, consistent with previous reports.[32] In the present study, ICV infusion of candesartan also partially inhibited Ras, p38 MAPK, ERK, and caspase-3 in the RVLM of SHRSP. The degree of the depressor effect of the Ras inhibitor on MBP in SHRSP was almost half that in WKY. These results suggest that AT_1R-activated caspase-3 acting through the Ras/MAPK/ERK pathway in the RVLM is one of the major pathways through which MBP, HR, and SNA are increased and BRS is decreased in SHRSP.

Another intriguing finding of the present study is that the apoptotic proteins Bax and Bad were activated, and the

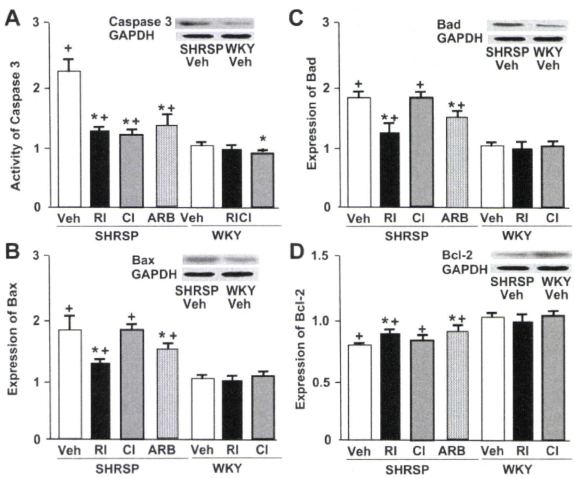

Figure 4. Activity of caspase-3 (A) and expression of Bax (B), Bad (C), and Bcl-2 (D) in the RVLM on day 14 in SHRSP and WKY treated with vehicle (Veh), Ras inhibitor (RI), caspase-3 inhibitor (CI), or ARB (n=5 for each). *$P<0.05$ vs Veh in each strain. +$P<0.05$ vs Veh-treated WKY. Activity and expression are shown relative to that in Veh-treated WKY, which was assigned a value of 1. Data are shown as mean±SEM.